# Enhanced performance of novel hydroxyethyl cellulose grafted amide-based microcapsules by catalyzed interfacial polymerization: Synthesis, characterization, and theoretical studies

El Yousfi Ridouan, Achalhi Nafea, El Ouardi Youssef, Lamsayah Morad, El Barkany Soufian, Laatikainen Katri, El Idrissi Abderahmane



**DOI:** 10.1016/j.reactfunctpolym.2023.105533

# Enhanced performance of novel hydroxyethyl cellulose grafted amide-based microcapsules by catalyzed interfacial polymerization: Synthesis, Characterization, and Theoretical Studies

Ridouan El Yousfi *[a], Nafea Achalhi[a], Youssef El Ouardi*[b], Morad Lamsayah[a], Soufian El Barkany[c], Katri Laatikainen[b], Abderahmane El Idrissi*[a]

[a] *Laboratory Applied Chemistry and Environmental (LCAE-URAC18), Faculty of Sciences of Oujda, Mohamed 1st University, 60000 Oujda, Morocco.*

[b] *Lappeenranta-Lahti University of Technology LUT, school of Engineering Science, Department of Separation science, Yliopistonkatu 34 FI-53850 Lappeenranta, Finland.*

[c] *Laboratory of Molecular Chemistry, Materials and Environment (LMCME), Department of Chemistry, Faculty Multidisciplinary Nador, Mohamed 1st University, P. B. 300, Nador 62700, Morocco.*

**Corresponding authors. E-mail addresses* ab.elidrissi@yahoo.fr *(Abderrahmane El Idrissi),* Red1elyousfi@gmail.com *(El yousfi Ridouan),* youssef.el.ouardi@lut.fi *(El ouardi youssef).*

**Abstract**

Due to their biodegradability, biocompatibility, non-toxicity, and affordable manufacture from renewable resources, hydroxyethyl cellulose (HEC) and its derivatives have gained growing interest in a variety of sectors. In light of this, HEC and HEC-branched-amide (HECA) were used to develop new polyurethane and polycarbamoyle amide-based microcapsules. The structure of the HECA prepolymer and the elaborated microcapsules were examined using FTIR, NMR, DRX, DLS, SEM, TGA, and Zeta Potential. The Polycarbamoyle amide microcapsules were prepared by catalyzed interfacial polymerization between the diisocyanate and the amide group of HECA. The enhanced kinetics of carbamoyle amide membrane formation using copper catalyzed polymerization is shown to have an advantage in maintaining the characteristics of the microcapsules. The stability and resistance of the microcapsules under temperature and pH conditions were also investigated. Due to strong bidentate interactions between the carbamoyle amide groups in the membrane, the microcapsules based on these groups display great stability in front of the microcapsules made of polyurethane. Theoretical studies have demonstrated these interactions, while the FT-IR results have supported these findings. The obtained results prove a positive enhancement in limonene encapsulation efficiency as the amount of carbamoyle amide groups within the membrane of the microcapsules is increased, reaching a maximum value of 96.84%. The shape has developed into a perfectly spherical, hard shape with a typical microcapsule diameter of 9 μm.

***Keywords:*** Hydroxyethyl cellulose (HEC); HEC amide; Microcapsules; Microencapsulation, Controlled release; Catalyzed interfacial polymerization.

## 1. Introduction:

The process of encapsulation is mostly employed for the stability and controlled release of substances having considerable activities, such as anti-cancer, antioxidant, antibacterial, and antifungal [1]. Encapsulation has recently been identified as a significant method used in many industries, including pharmaceutics, cosmetics, food ingredients and medication delivery. It is based on the encapsulation of liquid, solid, or gaseous compounds in thin-walled micro-particles called microcapsules.

Encapsulation has been developed using a variety of techniques, including interfacial polymerization. Since the mide-20th century, this method has been frequently employed. It started in 1959 with Beaman et al [2], who succeeded in producing polyamide-based microcapsules, and in the same year, Wittbecker and Kartz [3] elaborated microcapsules based on polyurethane using the same technique. In the 1960s, several groups [4, 5] identified interfacial polymerization on the surface of emulsion droplets, leading to microcapsules composed of liquid droplets enclosed in a solid polymer membrane. Interfacial polymerization has many advantages, including distinct properties in size distribution, rapid reaction rate, mechanical efficiency, flexibility, and biodegradability of synthesized items such as Polyurethane-urea [6]. Polyurethane-urea is a special polymer, which is distinguished by a large number of valuable properties. Due to its structure, this type of polymer presents excellent biodegradability, biocompatibility and very good mechanical strength [7, 8]. Retention of its high temperature resistance, abrasion resistance, resistance to ozone and oxidation, resistance to fungi, and high resistance to moisture, presents an excellent choice for the encapsulation of active ingredients [9, 10]. Among the most widely used methods for the production of polyurethane-urea microcapsules by interfacial polymerisation is the use of isocyanates as a cross-linking agent. The shell formation is due to the reaction between the -NCO groups of the isocyanate and the active functions of the amine or alcohol present in the aqueous phase of the emulsion system [11]. The type and amount of monomer used may control the (mechanical/physical) properties of the resulting polymer [12]. Sources of active groups may have different chain lengths and chemical structures and, consequently, different steric hindrance and reactivity, which strongly affect the morphology and thickness of the microcapsules shells [13]. The interactions developed between the groups that constitute the membrane of the microcapsule have appeared as the key factors affecting the properties of microencapsulation. The diffusion of coated molecules is slower in the presence of higher crystallinity, which may be due to the potency of electrostatic interactions and hydrogen bonds. The increase of those interactions inside the membrane favors the protection of essential oils against degradation caused by environmental factors [14, 15]. For that reason, several modifications on the polyurethane chains have been developed by controlling the length of both regular and flexible chains; this control leads to the balance of strength and toughness. Moreover, changing the types of reagents that react with the isocyanate function affects the properties of the polymer. The classical reagents are the diols forming the urethane zones and the diamines that form the urea ones; other reagents can replace both. [16-18]. The microcapsules sanitized by polyamide–polyurea shell showed a thicker membrane with excellent mechanical properties and the ability to have a porous membrane [19]. The hard and soft-segmented PU microstructure can also be adjusted by injecting polyester or polyether into the chain. The drug molecules encapsulated in these carriers displayed a fast rate of degradation, a much higher encapsulation performance, and a longer and more regulated release profile [20-22]. Other developments of urea and urethane groups have been rationalized as the production of poly (urea–formaldehyde). The integration of these two groups has significantly increased the thermal stability and mechanical properties of the microcapsules [23]. In addition, the modification of the microcapsules with biuret functions has improved the healing effect of the microcapsules triggered by water immersion, thus enhancing corrosion protection in the damaged area of the coating [24]. In accordance, when cellulose derivatives were introduced into the domain structure of PU, the mechanical properties were improved due to the reinforcing effect. In addition, cellulose esters are being explored for their applications in the field of controlled release systems due to their well-established preparation processes and biocompatibility [25]. The interaction between carbohydrates such as cellulose derivatives and the PU components results in different properties of the polymer. Carbohydrates can be used as cross-linking agents in the PU network due to the presence of several hydroxyl groups that can react with isocyanate groups. The cross-linked network thus formed can be applied for loading drugs inside the PU matrix or membrane [26]. The hydroxyethyl cellulose is among the most widely used hydrocarbons in various biomedical and pharmaceutical applications because it is inexpensive, non-toxic, biodegradable, and biocompatible [27].

In the present work, we successfully developed a new approach to designing two classes of advanced microcapsules. These microcapsules were synthesized using hydroxyethyl cellulose (**HEC**) or hydroxyethyl cellulose-branched-amide (**HECA**). The elaboration of isocyanate with **HEC** was for the aim of preparing the polyurethane microcapsules **PU**. On the other hand, **HECA** bestowed three Carbamoyle amide-based microcapsules $\mathbf{PC_{0.5}}$, $\mathbf{PC_{1}}$, and $\mathbf{PC_{1.5}}$ relative to the rate of substitution degree **DS** of amide groups in the **HEC** used (**DS**=0.5, 1, and 1.5, respectively).

The main purpose of those microcapsules' diversity will be debated in the framework of the stability and the performance toward various conditions, for instance, the high temperature resistance, kinetics of liberation, and the conservation of microcapsule characteristics during the synthesis process. In light of the literature interest concerning the effect of hydrogen interactions and their significant impact in improving membrane performance [28-30], the focus of this comparison will be to demonstrate the positive effect of the types of interactions created by the carbamoyle amide group in front of the polyurethane.

It is worth stating that the reactions of amide and isocyanate functions were first mentioned in 1884 [31]. This reaction requires prolonged exposure to high temperatures (above 110°C). Furthermore, the coupling between an amide and the isocyanate function at room temperature under the presence of a copper catalyst was reported recently [32]. However, this type of reaction was never applied to construct a high polymer chain. Thus, in our case, Carbamoyle amide-based chain membrane was constructed for the first time in this work. This reaction was well fulfilled by a catalyzed interfacial polymerization, which would drastically improve the reaction conditions in terms of the time required and yield.

## 2. Experiments:

### 2.1. Materials:

2-hydroxyethyl cellulose (**HEC**, Mn=90.000g/mol, DS=1.5), diphenylmethane4,4′ diisocyanate (**MDI**), Polyethylene glycol 600 (**$PEG_{600}$**) for synthesis, 2-bromoacetamide 98% , dibutyltin dilaurate (**DBTDL**) , copper (II) chloride dehydrate ≥99.0% **$CuCl_2 \cdot 2H_2O$** , N,N-dimethylformamide ACS reagent ≥ 99.8%, ethanol absolute ≥ 99.8%, n-hexane ≥ 99.0%, were purchased from sigma Aldrich.

### 2.2. Limonene Extraction:

In this study, limonene was extracted and used as organic phase during the preparation of microcapsules. The extraction process was carried out by hydrodistillation using Clevenger type apparatus. Briefly, 250 g of the fresh peels from C. aurantium fruits were introduced into a flask. The extraction temperature was maintained between 75°C and 80°C for 3 hours. Then, the essential oil was obtained and dried over anhydrous $Mg_2SO_4$.

### 2.3. Synthesis of HEC-branched-amide prepolymer ($HECA_X$):

The **$HECA_X$** prepolymer was synthesized by dissolving 1 g of **HEC** (13.87 mmol) in 15 ml of DMF. Depending on the desired degree of substitution of branched amide groups in **HEC**

(**X=DS =0.5; 1 or 1.5**), different amounts of **2-bromo-acetamide** were added. Then, the mixture was allowed to stir at room temperature until a transparent solution appeared. After this, the melange was maintained under stirring and heated at 60°C for 3 hours. The various **HECA$_x$** obtained (**HECA$_{0.5}$** DS= 0.5; **HECA$_1$** DS=1; **HECA$_{1.5}$** DS=1.5) were precipitated in a large excess of cold ethanol, filtered under vacuum, and washed thoroughly with cold ethanol. Afterward, they are stored in a desiccator in the presence of $P_2O_5$ for a week. Finally, white products with high water solubility were recuperated. The schematic synthesis of hydroxyl ethyl cellulose-amide (HECA) is shown in **Fig.1**.

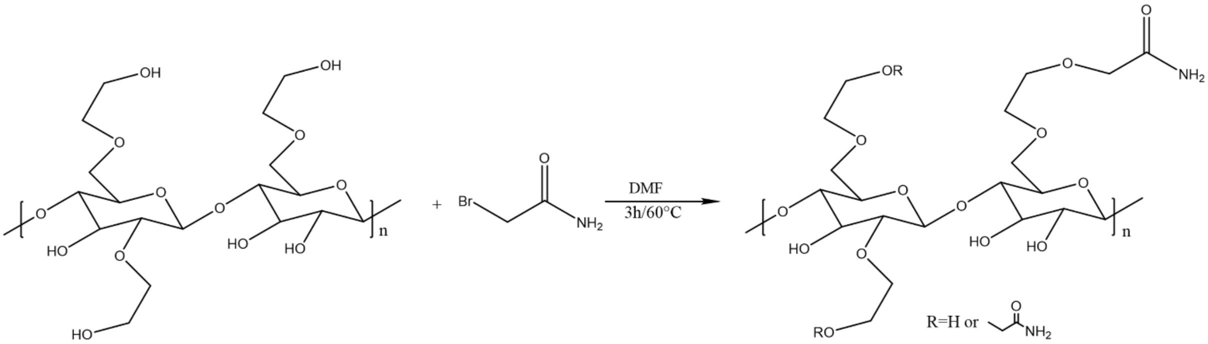


**Fig.1.** Schematic synthesis of hydroxyl ethyl cellulose-amide.

### 2.4. Microcapsules Preparation:

Firstly, O/W emulsion solution was prepared as follows: the organic phase (16ml of **limonene** + 8 ml of the **MDI** disocyanate) was mixed with 100 ml of water and 3 wt. % **SDS** (relative to the organic dispersed phase) [33], and vigorously agitated (9000 rpm) for 3 minutes at room temperature. Afterwards, the emulsion was divided into four polymerization reactors and heated to 60 °C under stirring (500 rpm).

Based on the prior emulsion prepared, four synthetic paths were performed to gather different types of microcapsules (Polyurethane: **PU**, and Polycarbamoyle amide: **PC**), depending on the protocol and the nature of the reagents used, which will be further described below.

**Table 1.** The specific parameters adopted in the study.

| **Reactor number** | | **n (PEG) mmol** | **n (HEC) mmol** | **n ( HECA$_X$) mmol** | | | **n isocyanate mmol** |
|---|---|---|---|---|---|---|---|
| | | | | **HECA$_{0.5}$** | **HECA$_1$** | **HECA$_{1.5}$** | |
| **1** | **PU** | 2.9 | **2.3 (0.65g)** | - | - | - | 9.8 |
| **2** | **PC$_{0.5}$** | 2.9 | - | **2.3 (0.8 g)** | - | - | 9.8 |
| **3** | **PC$_1$** | 2.9 | - | - | **2.3 (0.9g)** | - | 9.8 |
| **4** | **PC$_{1.5}$** | 2.9 | - | - | - | **2.3 (1 g)** | 9.8 |

### 2.4.1. Synthesis of Polyurethane-based Microcapsules (PU):

The **$PEG_{600}$** (2ml, 2.9 mmol) and **DBTDL** were added to reactor 1, containing the emulsion. The mixture was heated to 60°C while maintaining the same stirring for one hour. After that, 0.65g (2.3 mmol) of **HEC** dissolved in 10mL of distilled water was slowly added to the above reaction mixture while maintaining the same conditions for two additional hours. After centrifugation, the solid obtained was washed with a mixture of ethanol and distilled water (30/70), then washed twice with water to remove residual reagents to get the desired Polyurethane **PU** microcapsules.

### 2.4.2. Synthesis of Carbamoyle amide-based Microcapsules (PC):

The three reactors left were used to prepare the carbamoyle amide microcapsules. Briefly, the PEG was added in the presence of DBDTL into each reactor emulsion solution. The mixtures were heated at 60°C for 1 h. Then, each of the three previously prepared **$(HECA)_x$** prepolymers were added as follows: **$HECA_{0.5}$** into reactor 2, **$HECA_1$** into reactor 3, and **$HECA_{1.5}$** into reactor 4 (The molar quantities used are summarized in **Table.1**). After this, $CuCl_2$ (1% mole relative to the isocyanate quantity) was added to each mixture and heated at 60 °C for two additional hours. After centrifugation, the solid obtained by the three reactions where each washed with a mixture of ethanol and distilled water (30/70, v: v), then washed twice with water to remove residual regents.

Finally, three different microcapsules were obtained depending on the initial **$HECA_x$** used: **$PC_{0.5}$** for **$HECA_{0.5}$ (reactor 2)**; **$PC_1$** for **$HECA_1$ (reactor 3)**; and **$PC_{1.5}$** for **$HECA_{1.5}$ (reactor 4).**

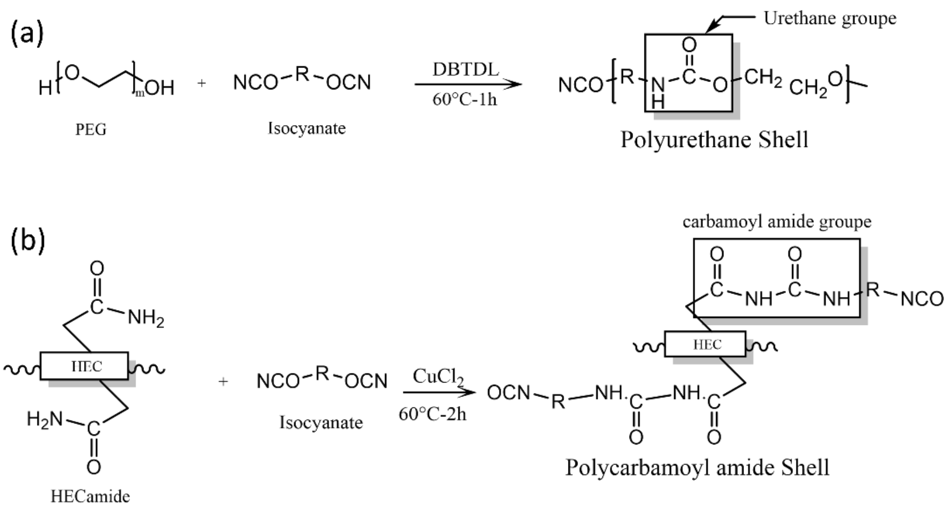


**Fig.2.** Schematic reaction synthesis of polycarbamoyle amide microcapsules (PC): **(a)** formation of polyurethane zone in the first step **(b)** formation of carbamoyle amide in the second step.

## 3. Results and discussion:

### 3.1. Oil characterization:

The CPG Analysis of the essential extracted oil (**Fig.S2** in supplementary document) revealed three major constituents: D-Limonene (96.34%), Dimethyl phthalate (2.14%), Beta-Myrcene 1.15). This is shows that limonene is the majority compound.

### 3.2. HECA prepolymer characterisations:

#### 3.2.1. FT-IR analysis of the HECA:

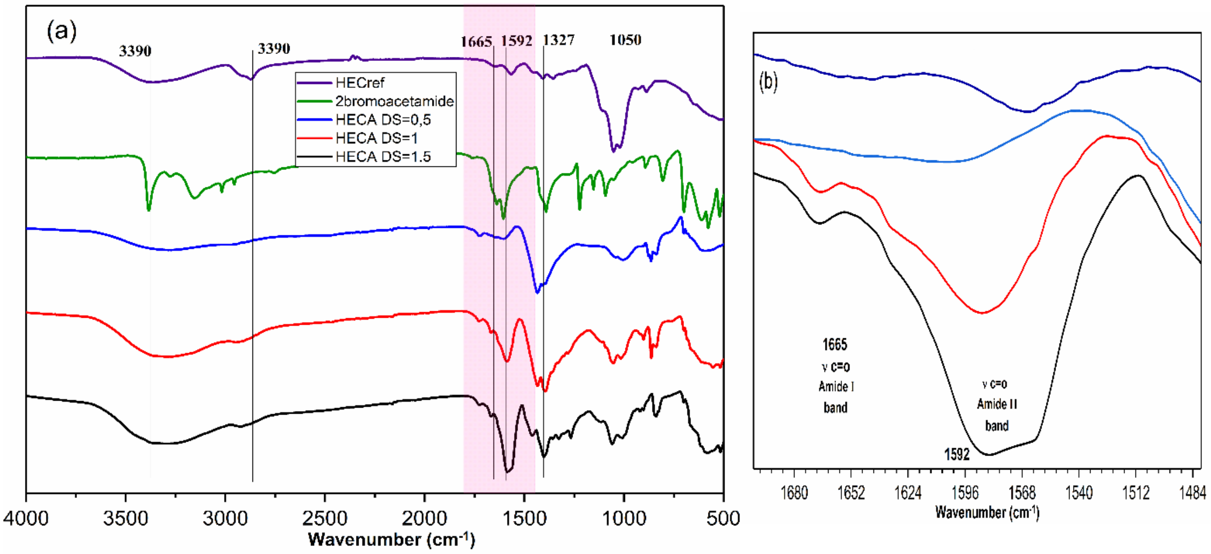


**Fig.3. a)** FT-IR spectra of Hydroxyethyl cellulose (HEC) and Hydroxyethyl cellulose grafted by amide (HECA) with deferent DS (0.5, 1, and 1.5). **b)** The typical bands of the C=O vibration of the amide group.

**Fig.3a** shows the FTIR spectra of HEC before and after modifications with deferent DS (0.5, 1 and 1.5). The absorption characteristic band of the OH elongations located around 3400 $cm^{-1}$ as well as the one at 1050 $cm^{-1}$ attributed to the units (-CH-O-$CH_2$) of HEC [34] were drastically decreased in the case of the modified HEC, however, CH bands were notably increased. In addition, the appearance of the new absorption bands in modified HEC at 3390 $cm^{-1}$ is attributed to the vibrations of the amide -$NH_2$ that proves the grafting reaction success. Moreover, the bands around 2920–2881 $cm^{-1}$ are attributed to the symmetric and asymmetric CH vibrations. Besides, the intense band appearing at 1592 $cm^{-1}$ in **Fig.3b**, is associated to the absorption of the C=O stretching vibration of the amide II group. On the other hand, the peak located at 1665 $cm^{-1}$ reveal the presence of C=O stretching vibration of the amide I group [35-37]. Furthermore, the peak detected at 1327$cm^{-1}$ corresponding to the band vibration of the C-N stretching [38]. Thus, judging by the above interpretations, it is recognized that the amide groups of 2-bromo-acetamide has been grafted on the cellulose backbone during the reaction.

### 3.2.2. $^{1}H$ NMR spectra of the HECA:

**Figure.4** shows the $^{1}H$ NMR spectra of HECA (DS=1.5). The peaks of the methylene protons on α of different hydroxyl groups are positioned between ~3.5 ppm and ~3.6 ppm, and those attached to the carbon (C6) of the cellulose backbone report signals over ∼3.49 ppm. In addition, the broad-cycle protons of the cellulose chain are found in the area of 2.8-5.5 ppm. On top of that, the peaks at 3.79 ppm are referred to α proton (2) which is linked to the carbon atom of the acetamide group. Not to mention the intense signal situated at 3.78 ppm that is tied to the methylene protons belonging to 2-bromoacetamide. The substitution degree of HEC by amide functions was estimated at ∼1.5.

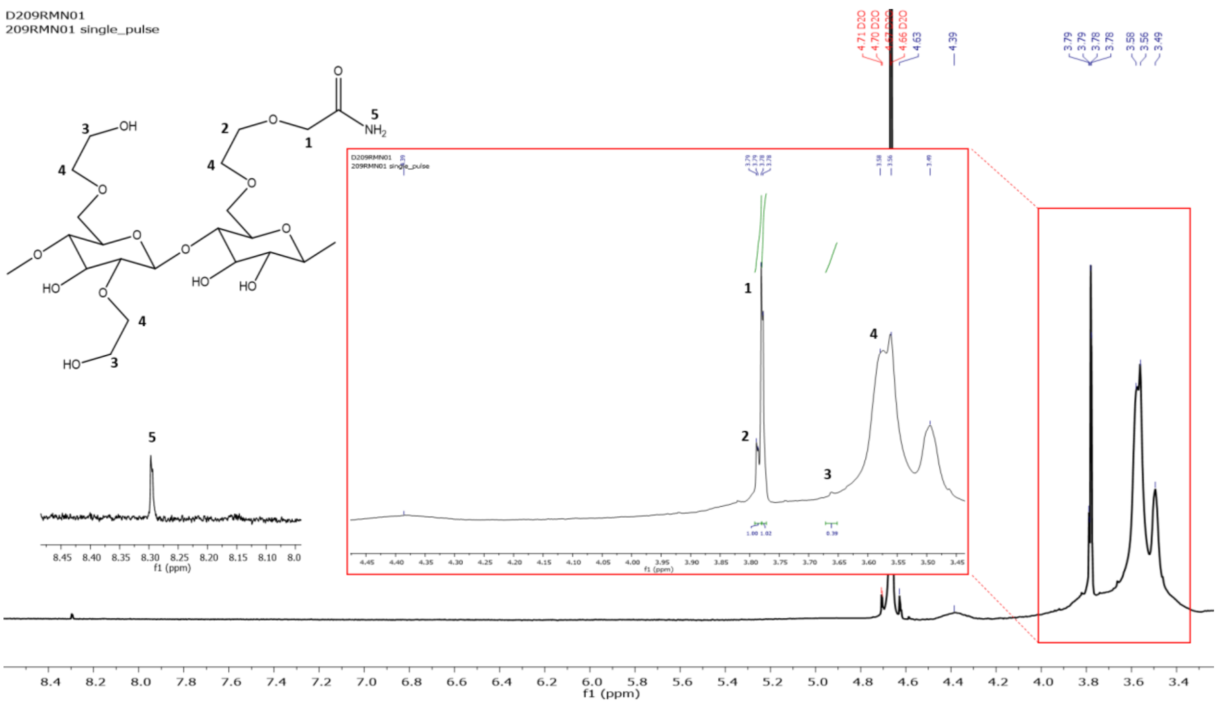


**Fig.4.** $^{1}H$ NMR spectra in $D_2O$ of HEC-branched-amide prepolymer (HECA).

### 3.3. Microcapsules characterisation:

### 3.3.1. FT-IR Characterization of Microcapsules:

The FT-IR spectra suggest the successful completion of the polymerization by the disappearance of the isocyanate absorption bands at 2200–2230 $cm^{-1}$.

The vibration assigned to 1015 $cm^{-1}$ corresponds to the stretching mode of (C-O-C) ether group, which originates from $PEG_{600}$ and HEC materials. Moreover, C-H stretching vibrations are assigned at 2926 and 2856 $cm^{-1}$ **(Fig.5a)**. The N-H of the primary amides stretches between 3300 $cm^{-1}$ and 3440 $cm^{-1}$ [39]. As presented in **Fig.5b**, two principal bands were detected, one at 3300 $cm^{-1}$ assigned to the associated hydrogen-bonded NH groups and a second one at about

3440 cm$^{-1}$ assigned to the free NH groups [40]. The high intensity of the band at 3300 cm$^{-1}$ in the case of **PC$_{1.5}$** microcapsules confirms the presence of hydrogen bonding interactions between the chains.

Additionally, the manifestation of Polyurethane zones in the microcapsules **PU** types exhibits two characteristic bands. The first can be observed at 1705 cm$^{-1}$. This peak is assigned to the free C=O group [41]. The second characteristic band can be found at 1715 cm$^{-1}$ which represents the Amide I (ν CO-N-H) [42, 43].

On the other hand, the formation of Carbamoyle Amide in the microcapsules PC$_{0.5}$, PC$_1$ and PC$_{1.5}$ types is confirmed by the existence of four characteristic bands. Primarily the free C=O group that appears at 1690 cm$^{-1}$ for all types [40]. Second, for PC$_{0.5}$ and PC$_1$, the Amide I (ν CO-N-H) bands are shown between 1640 and 1680 cm$^{-1}$, and for PC$_{1.5}$, between 1645 and 1680 cm$^{-1}$ [37, 41].

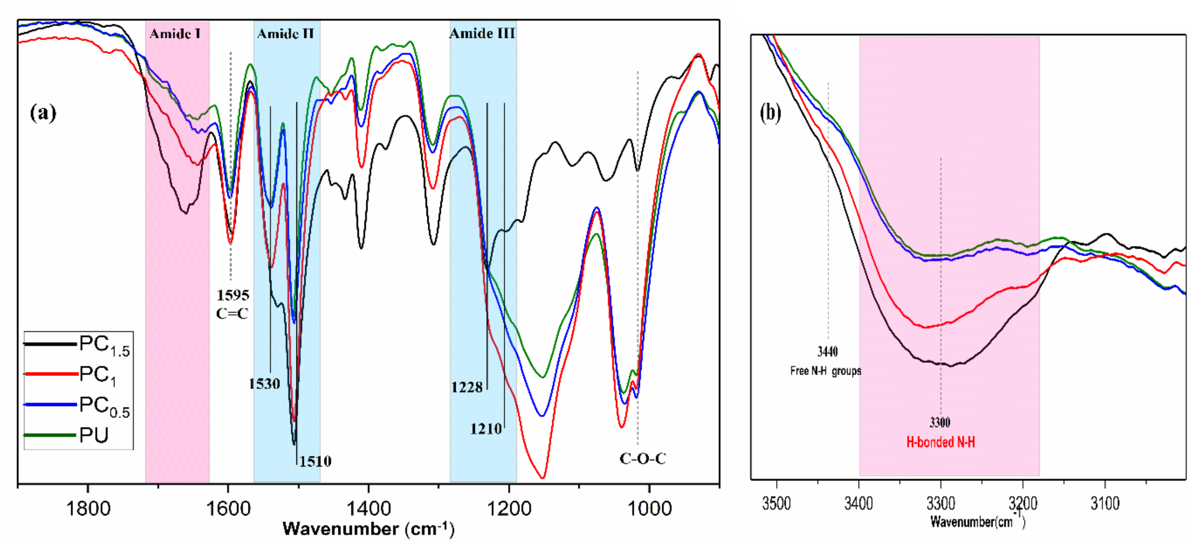


**Fig.5.** FT-IR Spectra of the different types of synthesized microcapsules.

The appearance of new Amide II (δ N-H + ν C-N) and Amide III (ν C-N + δ N-H) bands around 1510-1530 cm$^{-1}$ and 1210-1228 cm$^{-1}$, respectively, distinguishes Carbamoyle amide in microcapsules even more from PU types [44] [45]. The **Fig.6** summarizes all the above assignments.

### 3.3.2. FT-IR in depth discussions:

The difference between the types of hydrogen bonding formed by the urethane groups compared to those established by the Carbamoyle Amide groups plays a major role in the structural properties of the microcapsule membrane.

Starting from the free C=O group, the variation in the shifting values between various types of microcapsules justifies that **PU** are constituted by the urethane specimens, while **PC$_{0.5}$**, **PC$_1$**, and **PC1.5** are based on the Carbamoyle Amide class. Besides, the intensity gap shows the significance hydrogen bounding interaction within the Carbamolye Amide membrane.

As indicated in the above **Fig.5a**, the intensity of the amide I band of Polyurethane membrane **PU** is relatively lower in comparison to the three Carbamoyle amide based microcapsules types. Moreover, the intensity of the amide bands I and II increases in parallel with the Carbamoyle amide content in the membrane as follows: I(**PC1.5**)>I(**PC1**)>I(**PC0.5**). The high hydrogen linkage in these membranes also translates this.

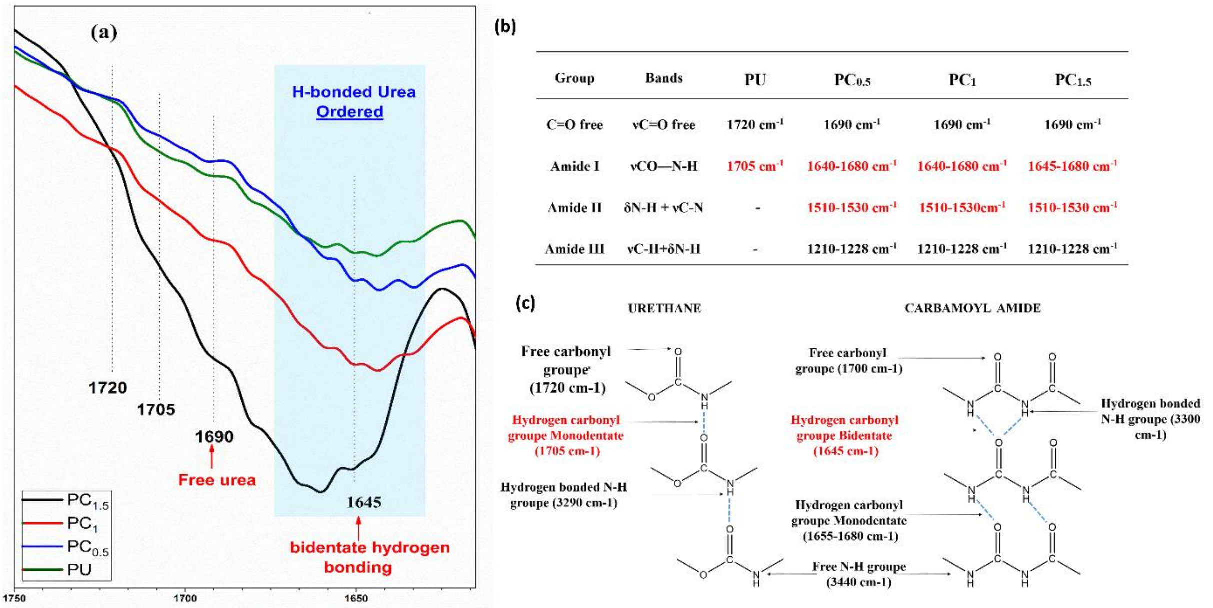


**Fig.6. (a)** FT-IR examination of the C=O region for different types of microcapsules.**(b)** and **(c)** band asignments for the polyurea carbonyl and N-H stretching modes. From reference [46, 47].

According to the literature review [41, 44], urea group's exhibit outstanding **bidentate interactions** or "dual" hydrogen bonding with each other [47]. What is even more intriguing, Carbamoyle amide possesses an enhancement of these types of interactions. In fact, It should be noted that the bidentate interaction generate a well-ordered character inside the membrane of the **PC1.5** microcapsules [48], which will favorably affect the stability of these microcapsules. This linkage between polymer chains is correlated with an increase in the density of hard domains self-associated by hydrogen bonding, which produces a physical cross-linking that increases the rigidity of the materials [49]. Additionally, the band associated with the crystalline carbamoyle-amide group (near to 1630 $cm^{-1}$) becomes more intense than the one associated with the amorphous carbamoyle-amide (1680 $cm^{-1}$) with the increase of the carbamoylamide group content in the membrane. This will gives a remarkable crystalline character to carbamoyl amide-based microcapsules [50]. However, on the other case the polyurethane chains are only linked by *monodantate* hydrogen bonds. The influence of these bonding modes within those materials on the properties and stability of the membrane will be further discussed in the remaining sections of the characterization.

### 3.3.3. Non Covalent Interaction (NCI) Study :

**Fig.7a** displays the findings of the calculations related to the interactions between the chains of carbamoyle amide constituting the membrane of **$PC_{1.5}$** microcapsules. By analyzing these results, a green and blue isosurface appears between the two units of the carbamoyle amide groups and specifically at the interface of a carbonyl group with the two nitrogen hydrogens, which indicates the existence of a van der Waals type attraction through the formation of two hydrogen bonds. This confirms the results of the FT-IR study, which showed an increase in the intensity of the hydrogen-bonded NH groups. The same interactions were noticed along both chains, creating good stability in the capsule membrane. This explains the high stability of this type of chain observed from the TGA analysis. A steric repulsive force between the two carbonyls of the same unit has been noticed (red parts).

### 3.3.4. Molecular Electrostatic Potential MESP:

Analysis of the electrostatic potential on the molecular surface can be used to predict points of activity on structures. The quantitative analysis of the molecular surface makes it possible to figure out the extreme points of the electrostatic potential; **Fig.7b, c**, and d represent these points with the corresponding calculated values. The positive (blue surface) and negative (red surface) potentials are distributed throughout the studied carbamoyle amide group structure. Their maximum electrostatic potential points (in yellow) are distributed along the carbon chain with the greatest value of approximately +52.42 kcal/mol observed near the two protons of nitrogen atoms. While the minimum points (in red) are distributed near the oxygen atoms due to their greater electro-negativities, with the greatest value of around-61.30 kcal/mol (**Fig.7b** and **Fig.7b)**.

By emitting the two groups units  in such a way as to have the minimum point of the first unit merged with the maximum point of the second one, the dimer found was optimized using the basis wb97xd / 6-311 ++ g (d, p). **Fig.7d** shows clearly an intersection of positive and negative electrostatic potential forming a favorable area to the hydrogen bonds; the distances of those bonds are also reported. All other unidentified minimum point values (-7.67 Kcal / mol) and maximum (+8.87 and 12.49 Kcal / mol) are generally small enough to have an influence on reactivity. The calculations revealed the existence of bidentate bonds between the two-carbamoyle amide groups. The stability of the membrane based on these groups is a result of these interaction models. Similar results have been found in the literature using the same calculation basis [49].

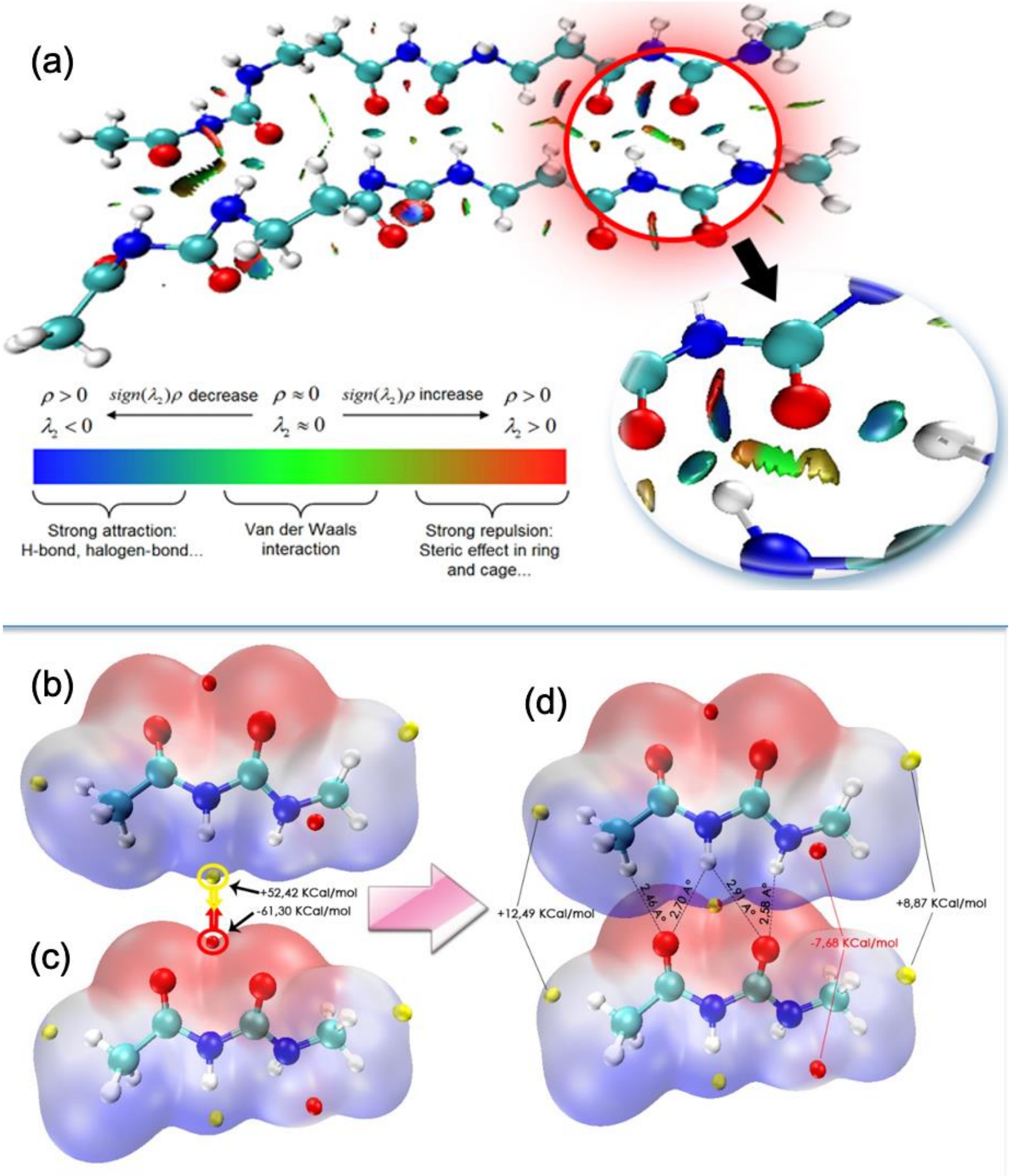


**Fig.7. (a)** Non Covalent Interaction (NCI) using the reduced gradient of the density (RGD). **(b), (c), a**nd **(d)** Minima and Maxima Point of Molecular Electrostatic Potential (MESP).

### 3.3.5. Isocyanate consumption rate:

Membrane formation kinetics is a process that is directly related to the rate of isocyanate group conversion (consumption rate). The Conversion calculations from the area of the isocyanate FT-IR peaks are presented in **Table.S2** on the supplementary document. **Fig.8a** and **8b** shows that the amount of isocyanate reacted with the amide groups increases remarkably in the presence of $CuCl_2$ as a catalyst. What is most crucial, the conversion of isocyanate reacted with the amide functions reached a conversion of 94% during 2h, which even exceeds the rate value when the isocyanate reacts with the hydroxyl group of HEC. As a result, the membrane kinetic formation of the carbamoyle amide-based microcapsules becomes faster and more efficient than the polyurethane-based microcapsules. This will favourably affect the properties of the microcapsules and the stability of emulsion droplets.

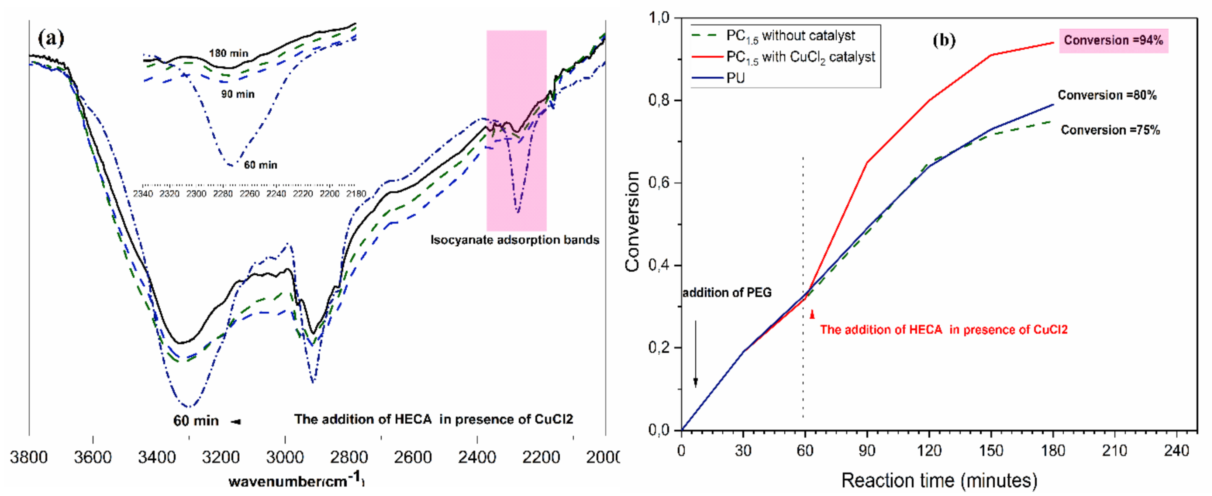


**Fig.8. (a)** chengement of the characteristic peak area to the isocyanate group during time of formation of the $PC_{1.5}$ microcapsules. **(b)** isocyanate conversion without and with the use of CuCl2 as catalyst for interfacial polymerization.

**3.3.6. The role of the $CuCl_2$ catalyst in the conservation of the microemulsion character during the polymerization:**

The main feature of the interfacial polymerization process lies within the preservation of the physicochemical properties of the polymerized micro-droplets as well as their distribution conservation. The membrane polymerization ratio plays a vital role throughout this survey.

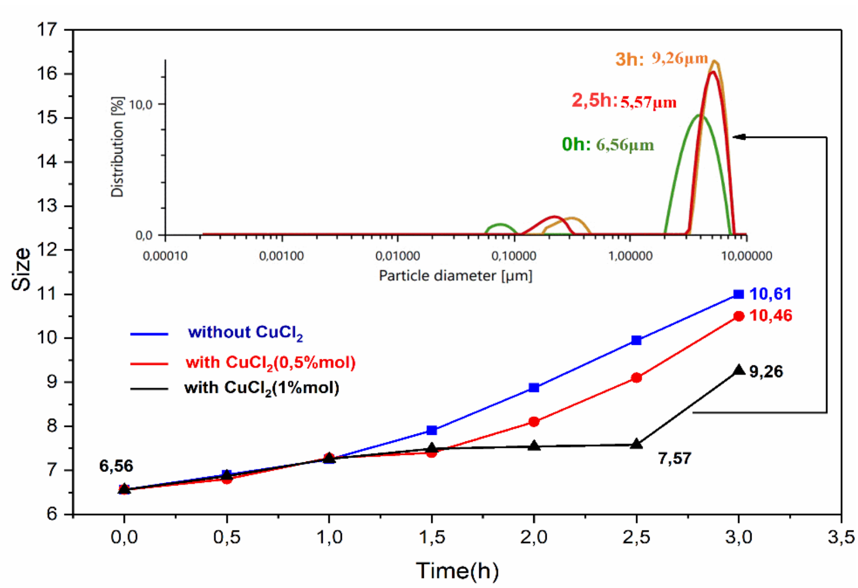


**Fig.9.** Size distribution of the micro-emulsion prepared without and with $CuCl_2$ during the time of $PC_{1.5}$ microcapsule synthesis.

**Fig.9** reveals that after the use of the catalyst $CuCl_2$ (1% mol), the **$PC_{1.5}$** microcapsules obtained by this procedure possess more similarity to the initial micro-droplets size, which is significantly superior in contrast to the lack of catalysis. In conclusion, the physicochemical properties of the micro-emulsion droplets were maintained during the establishment of the Carbamoyle amide membrane in the presence of $CuCl_2$, which is translated by the emulsion stability during the polymerization process of these groups.

### 3.3.7. $^1$H NMR spectra of the microcapsules:

The structure of the **$PC_{1.5}$** microcapsules was also analyzed in more detail by the $^1$H NMR technique, as shown in **Fig.10**. The signals corresponding to the protons of the $HEC_{amide}$ are clearly visible between 2.7 and 4.8 ppm. New signals appear and are attributed to aromatic isocyanate groups between 7 and 7.3 ppm,  while the signal at 3.75 ppm is assigned to the MDI methylene protons [51].

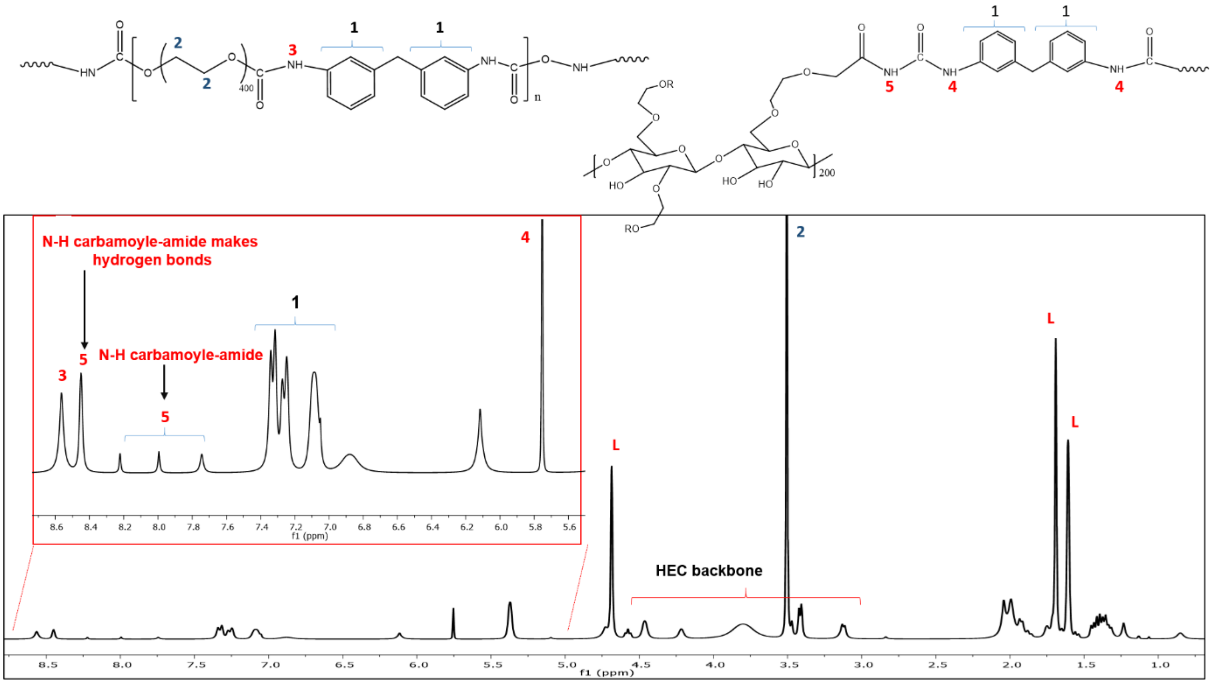


**Fig.10.** $^1$H NMR spectra in DMSO-d6 of $PC_{1.5}$ microcapsules (* L: characteristic peaks of limonene).

The PEG aliphatic segment protons are visible at 3.5 ppm [52, 53].  In addition, the appearance of signals attributed to the urea proton amide (5,7 ppm) demonstrates the -NH- protons next to the aromatic rings participating in the formation of the membrane of the capsules, while the signals of the urethane protons amide are visible at 8,6 ppm. Furthermore, the signal observed at 8.45 ppm indicates the formation of hydrogen bonds with the -NH of the carbamoyle amide group. [44, 51, 54]. Other peaks characterized by the limonene incorporated into $PC_{1.5}$

microcapsules were also located at 1.6 ppm, 1.7 ppm. 1.5 ppm, 1.9 ppm, and thus at 4.7 ppm and 5.4 ppm, demonstrating successful limonene encapsulation inside the microcapsules [55].

### 3.3.8. Loading capacity (LC) and encapsulation efficiency (EE) of Polyurethane and Carbamoyl amide based-Microcapsules:

The overall effectiveness of microcapsules is significantly influenced by the LC% and EE%. **Fig.S4** in the supplementary document, displays the LC% and EE% of the various types of microcapsules. According to the findings, an increase in the EE% and LC% typically coincides with an increase in the carbamoyle amide group amount inside the membrane. The maximum loading and encapsulation efficiency were demonstrated by the carbamoyle amide-based microcapsules $\mathbf{PC_{1.5}}$ (64% and 96.84%, respectively).

This excellent performance of $\mathbf{PC_{1.5}}$ microcapsules can be explained by the fact that the carbamoyl amide membrane provides perfect stability conditions for the microcapsules during the encapsulation process. The resistance of these capsules to protonation-deprotonation will be demonstrated by the zeta potential analysis that follow.

In addition, the rate of conversion of the isocyanate groups may also have an effect on the EE% [56]. A high and fast conversion value was seen in the kinetic analysis of the consumption of the isocyanate groups reacting with the amide groups when the $CuCl_2$ catalyst was present. This has a favorable impact on membrane development, and ultimately on EE%. The low conversion that results from the reaction of isocyanate with hydroxyl groups in the opposite situation and in the event of **PU** microcapsules, would result in the production of an unsuitable membrane.

In this case, isocyanates can also react with water in a solution to produce $CO_2$ bubbles. This results in a porous membrane and poor densification with low mechanical properties, which reduces the EE of **PU** capsules.

### 3.3.9. Zeta Potential study:

In order to investigate the stability differences of the microcapsules during the encapsulation process, the study of the colloidal system of **PU** and $\mathbf{PU_{1.5}}$ microcapsules was evaluated by the zeta potential at different pH, as shown in **Fig.11a**.

The zeta potential measurements determined the zero charge points (ZCP) of the two types of **PU** and $\mathbf{PC_{1.5}}$ microcapsules at 6.06 and 5.95, respectively. Thus, at pH 6, the surface of the microcapsules is positively charged while being negatively charged at higher pH. These surface charges can be generated by the protonation and deprotonation of NH groups in the urethane and carbamoyle amide group linkages [57]. It is clear that **PU** microcapsules exhibit a more significant charge modification due to the facility of protonation and deprotonation of the urethane groups on the surface; on the contrary, **$PC_{1.5}$** microcapsules show a resistance against this phenomene, which translates into a weak charge modification on the surface.

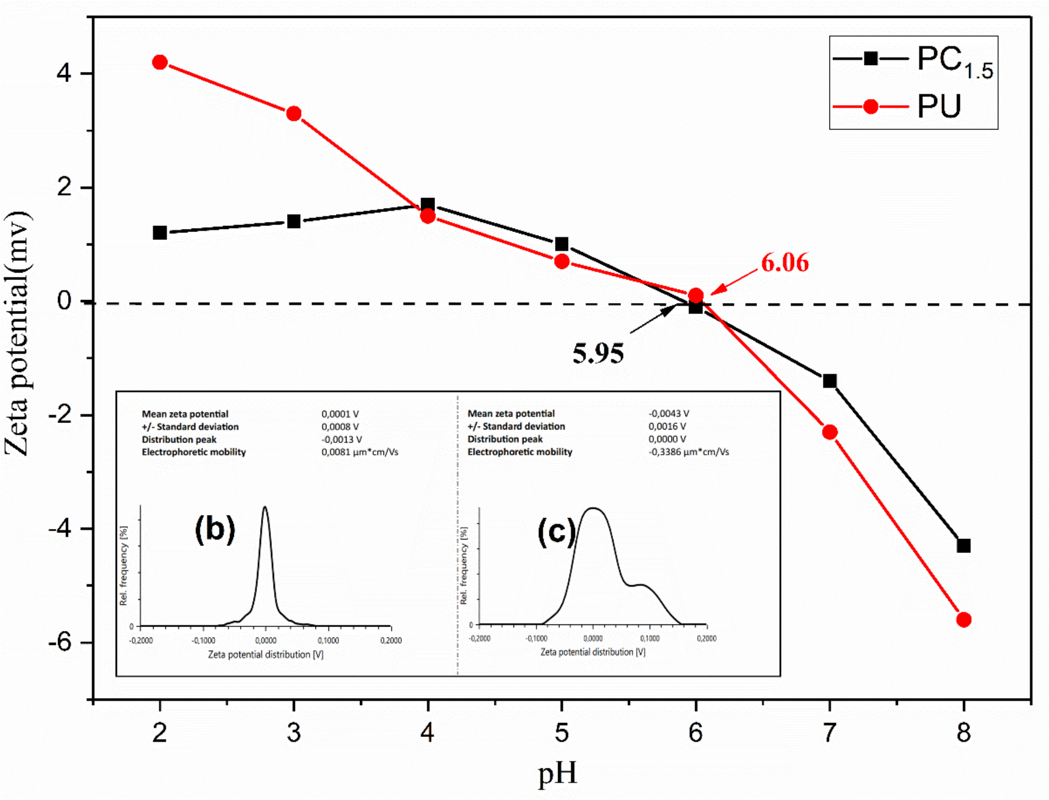


**Fig.11. (a)** Zeta potential analyse of $PC_{1.5}$ and PU microcapsules in various pH. **(b, c)** zeta potential distribution of $PC_{1.5}$ and PU microcapsules in pH=6.

Additionally, the **$PC_{1.5}$** microcapsules charge distribution at pH=6 (**Fig.11b**) displays the appearance of a single peak distribution, which amply demonstrates the neutrality of the microcapsule surface at this pH. In contrast, PU microcapsules (**Fig.11c**) displayed a two-peak distribution, indicating that positive and negative charges are compounded. At this ZCP, the surface always remains charged.

### 3.3.10. Microcapsules morphology:

#### 3.3.10.1. Optical microscope analysis:

The microcapsules morphology is among the most crucial factors towards the encapsulation process. Microcapsules with smooth surface and regular spherical shapes improves the effectiveness and liberation control of active ingredients.

The morphology of the manufactured **$PC_{1.5}$** microcapsules was analyzed using the optical microscope after making a suspension of these microcapsules powder in water, with different concentrations ( 0.5,1 and 5 mg/ml ) (**Fig.12 a,b,c** respectively). The optical microscope was used for observing the re-dispersibility of the powdered microcapsules. In addition, as anticipated, the microcapsules were dispersed after the addition of water, and thus, their re-dispersibility was clearly recognized [58].

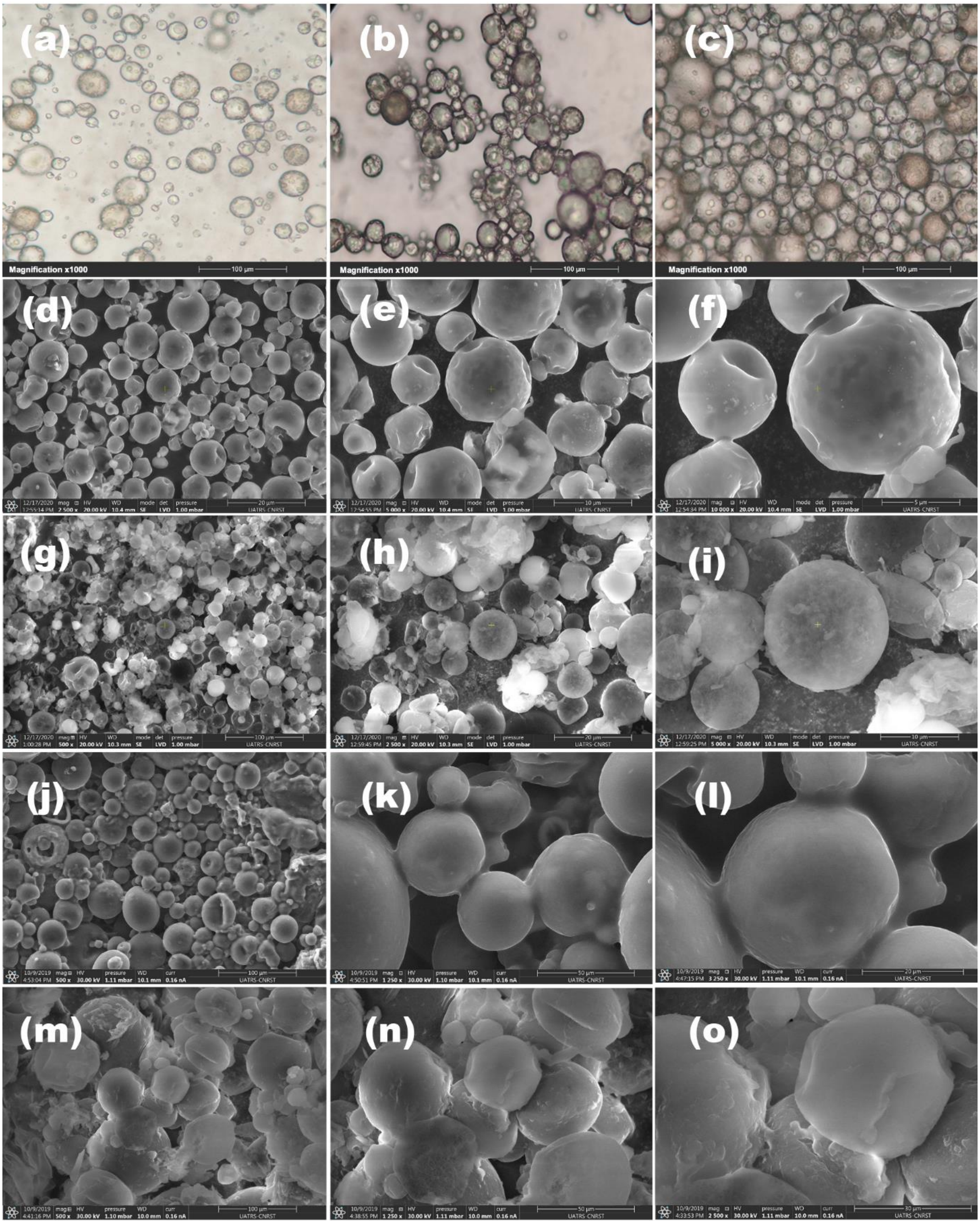


**Fig.12. a-b-c)** Optical microscope images of $PC_{1.5}$ microcapsules morphologies with different concentrations in an aqueous phase. **d to o**) SEM images of the morphology and structure of the different synthesized microcapsules after 6 month storage at room temperature. **(d-e-f)**: $PC_{1.5}$; **(g-h-i)**: $PC_1$; **(j-k-l)**: $PC_{0.5}$; **(m-n-o)**: PU.

### 3.3.10.2. SEM Analysis:

In order to compare the stability of the polyurethane and carbamoyle amide microcapsules obtained, they were stored at room temperature for six months and then analyzed with SEM [59]. The **Fig.12** reports magnifications of the various types of microcapsules. Overall, the microcapsules become smoother, well dispersed, and have an excellent spherical shape. These properties progress from polyurethane to carbamoyle amide as follows: **PU**<**$PC_{0.5}$**<**$PC_{1}$**<**$PC_{1.5}$**, which further proves the positive influence of **HECA** rather than **HEC**.

Furthermore, the size **(S)** of these spheres decreases in the same way (**SPU**>**$SPC_{0.5}$**>**$SPC_{1}$**>**$SPC_{1.5}$**). This is mainly due to the outstanding cross-linking of the carbamoyle amide chains that are more abundant in **$PC_{1.5}$** to **PU**. These microcapsules are very stable and preserve their spherical shape after 6 months at room temperature. This indicates that the polycarbamoyle amide membrane has enough strength to maintain its shape due to the high-energy interactions between the chains [60].

Moreover, these microcapsules overlap with each other in the case of polyurethane **PU** and the carbamoyle amide with less substitution degree **$PC_{0.5}$**. This phenomenon can be explained by the instability of the emulsion and the microcapsules during the first stage of the polymerization caused by the diffusion of an excess of the organic phase (limonene + isocyanate) through the membrane, which led to a certain flocculation between the microcapsules during the reaction [39, 61].

### 3.3.11. DLS analysis:

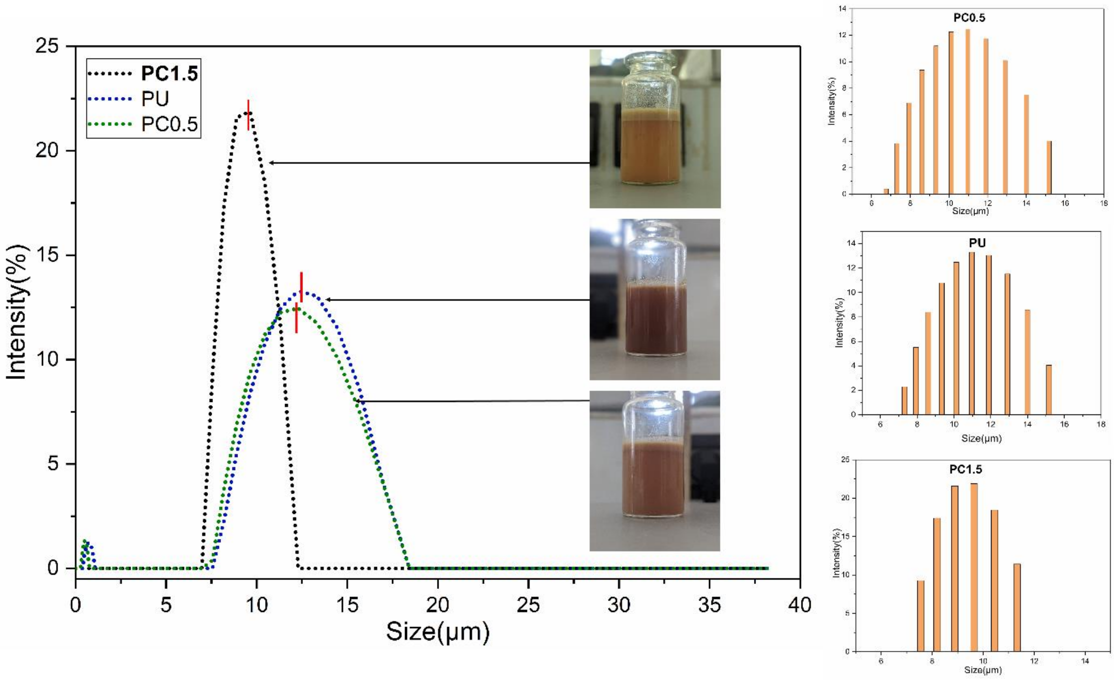


**Fig.13.** Particle size distribution of PU microcapsules.

DLS studies were used to characterize PU, $PC_1$ and $PC_{1.5}$ microcapsules in aqueous solution (**Fig.13**). The results show that PC1.5 microcapsules have the smallest size (9μm), while PU capsules have an average diameter of 13μm. Furthermore, the particle size distribution became small and the average particle size of the microcapsules decreased, apparently when the content of carbamoyle amide function in the microcapsules increased. A better degree of crosslinking in the capsule is achieved by increasing the amide bond, and a more compact capsule shell is obtained by increasing the crosslinking point. The particle size has therefore decreased instead.

### 3.3.12. EDS Energy Spectra Analysis:

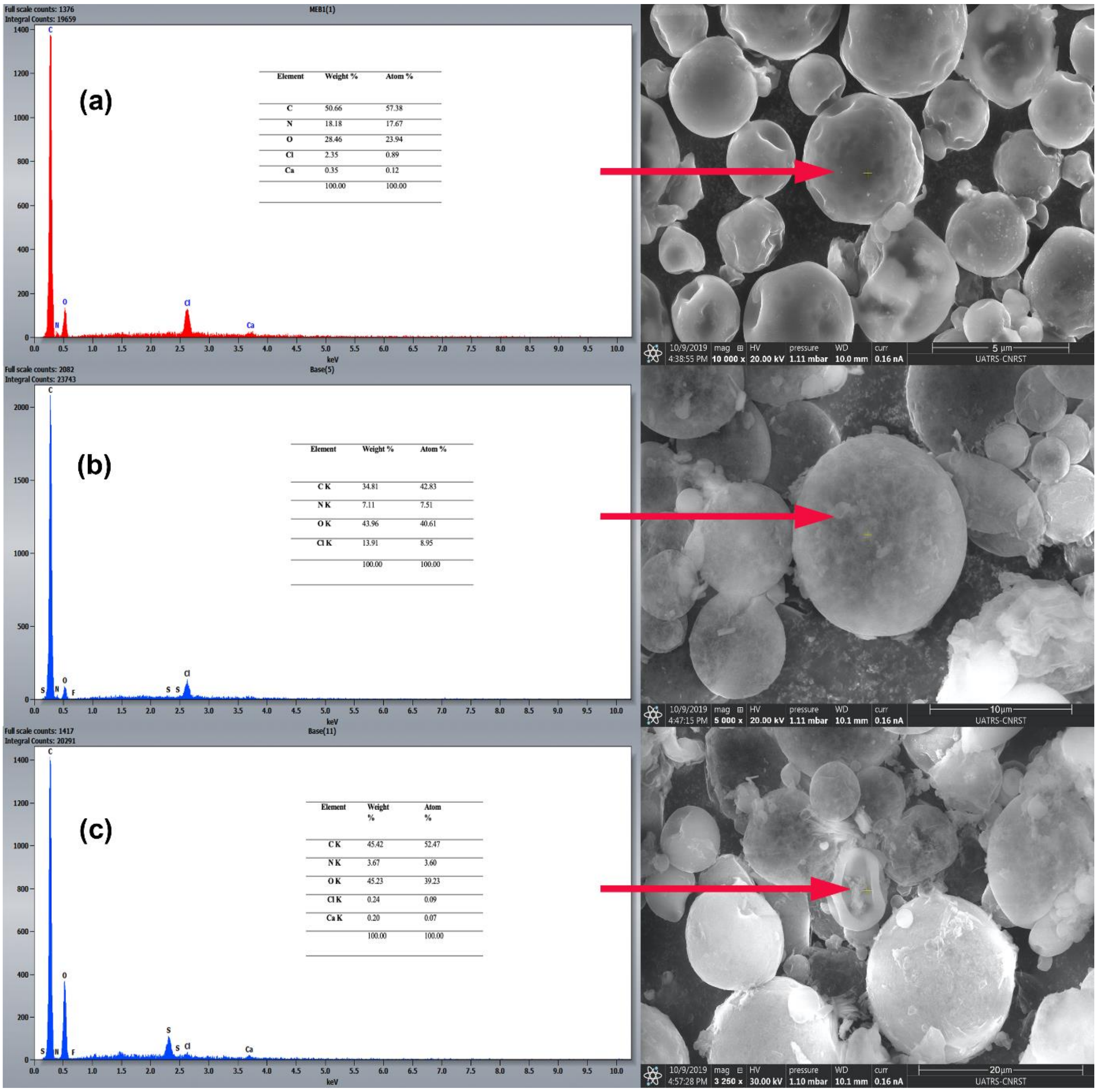


**Fig.14.** EDS results of **(a)** the external membrane of $PC_{1.5}$ microcapsules, **(b)** the external membrane of $PC_1$ microcapsules, **(c)** the internal membrane of $PC_1$ microcapsules.

In the **$PC_{1.5}$** microcapsule, which was predominantly made of carbamoyl functions, the C, N, and O components were 50.62, 18.18, and 28.46 wt%, respectively, as shown in **Fig.14a**. The outer surface of these capsules included more nitrogen than the **$PC_1$** microcapsules, whose membrane is made up of a lesser proportion of carbamoyl amide functionalities (34.81 wt% C, 7.11 % O, and 7.51 % N) (**Fig.14b**). This once more demonstrates the effectiveness of the reaction and the fact that a significant portion of carbamoyl amide functionalities are used to create $PC_{1.5}$ capsules.

According to EDS data in **Fig.14c**, the internal surface of **$PC_1$** microcapsules, which are made up of polyurethane cores produced by the reaction of isocyanate with PEG diol, is depicted. Theoretically, only extremely small amounts of nitrogen (N) should be present in this inner layer. The EDS results confirmed this theory. The nitrogen (N) concentration in the interior capsule shells was only 7.00 wt%, whereas it was 18.18 wt% outside the capsule shell.

The results of EDS analysing the internal and external surfaces of PU microcapsules demonstrate that the formation of the membrane was initially produced by the reaction of isocyanate with PEG, which forms the first layer of the capsule. Subsequently, the carbamoyle amide layer is produced to give the final shape of the capsule after the total consumption of diol and the addition of HEC-branched-amide prepolymer.

### 3.3.13. Thermal stability of microcapsules:

Thermal stability is deemed as one of the key factors in determining the properties of microcapsules and their practical application. TGA analysis allows the investigation of the thermal stability and thusly, the performances of microcapsules as the temperature rises. **Fig. 15a** reveals the thermo gravimetric analysis (TGA) of the membrane of **PU** capsules and **$PC_{1.5}$** shell with and without limonene.

The extreme weight loss witnessed in the polyurethane membrane **PU** between 100°C and 340°C is due to the decomposition process of the rigid polyurethane chains established by the unmodified HEC [62]. At this stage, the membrane loses 64% of its initial weight. Moreover, the decomposition of the soft segments of the polyol formed by the PEG occurs at higher temperatures [63]. On the other hand regarding **$PC_{1.5}$** microcapsules, the first slow mass loss starts at 150°C, which corresponds to the degradation of the poly carbamoyle amide chains that comes from the HEC amide, this small degradation ends at 360°C [59]. In this case, the weight loss was 26%, which is significantly lower in comparison to **PU** membrane. In conclusion, the thermal stability of carbamoyle amide microcapsules **$PC_{1.5}$**, is remarkably superior to polyurethane ones.

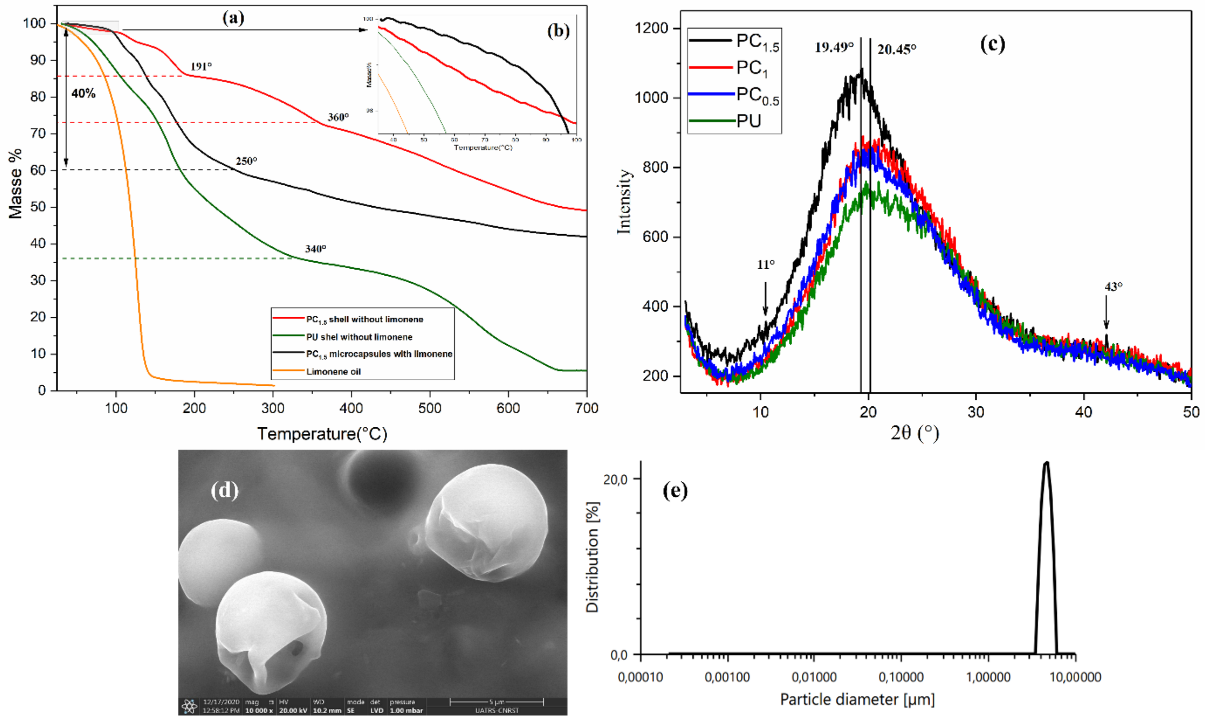


**Fig 15. a)** TGA curves of the microcapsules with and without limonene. **b)** The thermograph of the microcapsule in the first stage of heating (<100 °C). **c)** X-ray diffraction patterns of differs microcapsules shell. **d)** SEM image of a typical $PC_{1.5}$ microcapsule after storing for 15 days at 60 °C. **e)** Particle size of $PC_{1.5}$ microcapsules after storing for 15 days at 80 °C.

The **$PC_{1.5}$** microcapsules containing limonene exhibit good stability at temperatures below 150°C. After this, and up to 250°C, there was a definite weight decrease; these microcapsules lost 40% of their original weight. This proves that limonene was successfully encapsulated in the microcapsules and is consistent with limonene properties. The polycarbamoyle amide membrane, on the other hand, may also degrade at this temperature range. Due to the high shell protection of this type of microcapsules, the limonene encapsulated in the shells is likely decomposed and evaporated at higher temperatures.

It is essential to note that at temperatures below 100°C, the stability of **$PC_{1.5}$** microcapsules loaded limonene is more important than the membrane alone (**Fig.15b**). This proves that the combination of membrane and limonene improves thermal stability. Achieving good thermal stability of the microcapsules would postpone the direct evaporation of limonene inside the core and slow the polymer degradation process when heated [64, 65].

### 3.3.14. X-ray diffraction analysis:

Urethane-urea copolymers have the ability to form two types of segments: "soft" and "hard" in alternating and dispersed sequences. These two segments are thermodynamically incompatible and phase-separated resulting in discrete crystalline domains of the associated "hard" segments surrounded by a continuous amorphous phase of "soft" segments [41].

The X-ray diffractograms XRD in **Fig.15c** showed a large peak at 2θ = 20°. This peak is associated with the 4.69 nm distance of the intra-string segments that create rearrangement in certain areas of polymer (determined using Bragg's law). The separated domains are stabilized by inter-chain hydrogen bonds and are responsible for the mechanical properties of the materials [66, 67]. The increase in crystallinity between the **PU** samples is mainly evidenced by the increase in peaks located at 2θ =20.45°. In this case, the **PC$_{1.5}$** with the most intense peaks located at 2θ =19.49° and which has a shift of 1° compared to the other microcapsule types that possess a higher crystallinity index.

Furthermore, the powder diffractograms of **PC$_{1.5}$** also exhibit peaks at 2θ angles around 11°, and 43°, indicating some degree of crystallinity. These peaks are attributed to the scattering of polymer chains with regular interplanar spacing [67].

Since the peak intensity raises with the increase in the concentration of carbamoyle amide functions in the polymer membrane, it can be suggested that the excess of this group favours a certain mesomorphic (or crystalline) organization in the chains. These results show that the degree of crystallinity is controlled by the content of carbamoyle amide functions in the chains. This explains the reason why **PC$_{1.5}$** has the best stable crystalline and thus a thermal character compared to other architectures.

### 3.3.15. Effects of Temperature on the Release behaviour:

The stability of the four microcapsules **PU**, **PC$_{0.5}$**, **PC$_{1}$**, and **PC$_{1.5}$** was examined at three different temperatures values: 45, 60 and 80°C, during a 15 days period. The temperature effect on the release profile of each type of membrane was also investigated along with the weight measurements throughout this period. The results are shown in **Table.S3** of the supplementary document.

The weight of the microcapsules decreased as the heat treatment time increased. This is caused by the evaporation of the encapsulated limonene on the outside of the microcapsules under the effect of temperature. This weight drop was lower than 4.5% for all types of microcapsules at lower temperatures (60°C), however, at higher temperature (80°C), the **PU** microcapsules lost 28.95% of their weight, while **PC$_{1.5}$** microcapsules was about 19.9%. This once again proves the enhancement of the thermal resistance and the compactness of carbamoyle amide microcapsules compared to polyurethane microcapsules.

To further investigate the significant weight loss in the capsules, the **$PC_{1.5}$** microcapsules were observed by SEM after storage at 80 °C for 15 days. The **Fig.15d** shows the changes in morphology of the microcapsules. The capsules do not show any breaks in the membrane, which indicate that they release limonene by the diffusion phenomenon. In this case, limonene is released through the pores of the shells. Moreover, DLS analysis presented in figure **Fig.15e** reveals the decrease in size, which is due to the evaporation of limonene.

### 3.3.16. The release kinetics:

According to the previous reports in the literature [68], acidic environments lead to the urethane chains probable degradation. Additionally, this somewhat helped the release. For this, the release kinetics behavior for each type of capsule in an acidic medium (pH =4) was investigated at 25 °C and at a stirring speed of 100 rpm. The release of limonene depends on the envelope type, the morphology and the degree of solubility and protonation of the microcapsules in the acidic medium. The results are shown in **Fig.16a**.

The initial stage is accompanied by a rapid release of limonene that has accumulated on the surface of the microcapsule [69, 70]. The PU-type capsules release a very high amount of limonene at this stage, reaching up to 47%. In contrast, $PC_{1.5}$ types release only 18% of their content. This is mainly due to the high interactions within the membrane that prevent the leakage and release of limonene.

After 3 days, the second phase of release started. The results showed that PU-type microcapsules had the fastest release rate (releasing approximately 60% of the initial weight of limonene). On the other hand, the release slows down as the capsule membrane carbamoyle amide content rises. The $PC_{1.5}$ type has the slowest release (releasing only 25% of their initial content after 15 days). This is explained by the significant hydrogen interactions present in the membrane of this kind of microcapsule, and FT-IR analysis supports this. Furthermore, the zeta potential analysis demonstrated the resistance of $PC_{1.5}$ to the protonation in an acidic environment, allowing an excellent regulation of the active ingredient release.

### 3.3.17. Korsmeyer-Peppas mathematical model:

The release kinetics were also developed by applying the on the Korsmeyer-Peppas mathematical model described by the equation: $Kt^n = M_t / M_\infty$. The **Fig.16b** show the construction of the graph by using the Ln (Ct/C∞) as a function of Ln (t) provides the exponent (n) and the release constant (k). The fitting curves displayed a good linear correlation coefficient (R2 > 0.90), indicating that the Korsmeyer-Peppas mode could well characterize the release [71].

The n value achieved for the release exponents of the polyurethane PU types and of $PU_{1.5}$ (carbamoyle amide type) is in the range of 0.45< n < 0.85 (0.48 for PU and 0.51 for $PC_{1.5}$), indicating a combination of the coexistence of diffusion-controlled release of limonene and swelling-controlled release in the testing environment [72]. In addition, the release of limonene also occurred with no breakage or rupture of the microcapsule, as shown in the following figures **Fig.16c** [73].

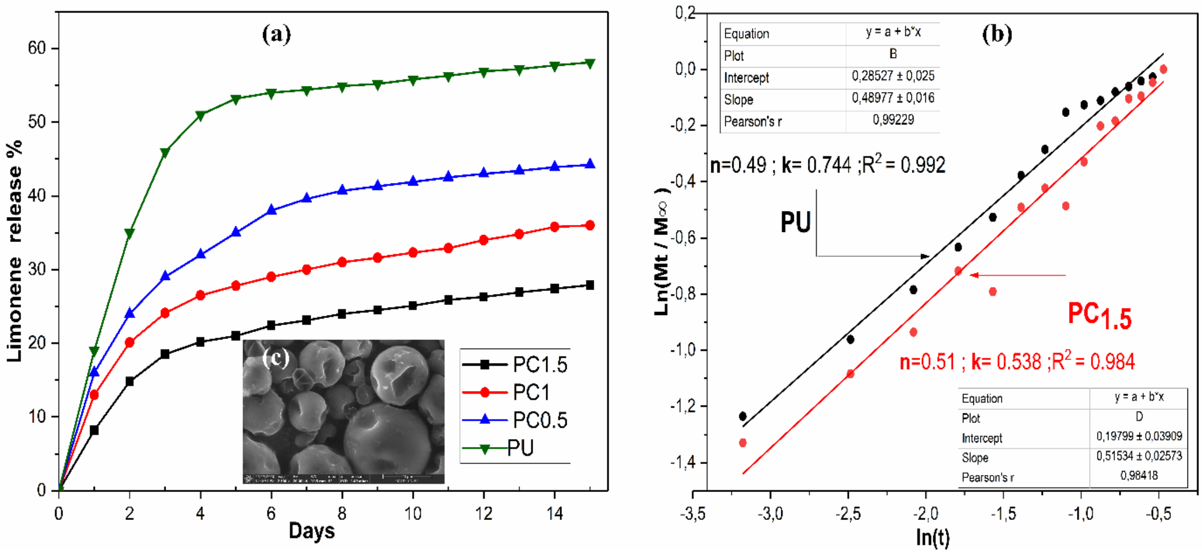


**Fig.16. (a)** The release profiles of different microcapsules under acidic pH =4. **(b)** Microcapsules diameter of $PC_{1.5}$ microcapsules after heat treatment. **(c)** SEM image of a typical $PC_{1.5}$ microcapsule after 6 months storage in acidic medium.

The rate constant K=0.538 of the $PC_{1.5}$ microcapsules based on carbamoyle amide is another feature. The average PU, in contrast, has a higher K=0.774. This demonstrates that the release of limonene from $PC_{1.5}$ microcapsules is substantially slower.

The bonds formed by the carbamoyle amide groups increase the polymer shell's stability and reduce limonene diffusion. The stability of polyurethane and polyurea groups is compared in the literature with similar findings [52]. Similar results are found in literature that compares the stability of polyurethane and polyurea groups [59].

## 4. Conclusion:

In this study, two major types of microcapsules based on polyurethane (PU) and polycarbamoyl amide (PC) were obtained with HEC and HECAx, respectively, to encapsulate limonene. The control of the DS of branched amide on HECA (x = 0.5, 1, 1.5) allowed the preparation of three types of microcapsules based on carbamoyle amide ($PC_{0.5}$, $PC_1$ and $PC_{1.5}$), which differ in their content of carbamoyle amide group. The purpose of this research is to compare the polycarbamoyle amide membrane performance to that of polyurethane and to show how the content of carbamoyle amide in the membrane affects the properties of the microcapsules. Through an interfacial polymerization that was copper-catalyzed, the polycarbamoyle membrane was developed. This novel approach enables the fast reaction of amide and isocyanate groups under normal temperature conditions. Due to the fast kinetics of membrane development, the microcapsules remain stable during synthesis and the emulsion properties are preserved.

The performance of the microcapsules is significantly improved by the presence of the carbamoyle amide group in the membrane. The results show the improvement in the performance of microcapsules based on carbamoyle amide as compared to polyurethane. The colloidal charge stability of carbamoyle amide microcapsules under various pH conditions is confirmed by zeta potential measurement. In addition, the slow mass loss of the polycarbamoyle amide membrane observed by TGA analysis confirms the thermal stability of this type of microcapsules. This stability is maintained by the high interactions among the carbamoyl amide groups in the membrane. The most significant interactions are the bidentate ones; this linkage was observed by FTIR analysis and supported by theoretical studies.

Based on these properties, the EE% increases as long as the content of carbamoyle amide groups in the membrane increase. The highest efficiency is shown by **$PC_{1.5}$** type microcapsules, which made with a high carbamoyle amide content (96%). The microcapsules in this instance are more rigid and exhibit a completely spherical shape, with an average diameter of around 9 µm.

**Credit authorship contribution statement:**

**El Yousfi Ridouan:** experimental part, characterization, investigation, writing, validation. **Nafea Achalhi:** characterization part, investigation, validation. **Youssef El Ouardi**: characterization part. **Morad Lamsayah**: theoretical study, writing. **Soufian El berkany**: supervision, formal analysis, correction. **Katri Laatikainen**: Formal analysis, data curation, validation. **Abderahmane El Idrissi:** supervision, formal analysis, writing-review and editing.

**Acknowledgments:** Special thanks to the head of the Chemistry department at FSO (Oujda) Abdelmonaem Talhaoui for Prof. Abdelmonaem TALHAOUI for making the analytical platform open for the researchers to do all the necessary analyses.

**Funding:** This research was partially supported and funded by Mohamed Ist University projects PARA I&II, CNRST and Etelä-Karjala Säästöpankki Foundation, Finland.

**Competing interests:** The authors declare that they have no known competing financial interests or personal relationships that could have appeared to influence the work reported in this paper.

## References


[1] N. Nikmaram, S.Y. Leong, M. Koubaa, Z. Zhu, F.J. Barba, R. Greiner, I. Oey, S. Roohinejad, Effect of extrusion on the anti-nutritional factors of food products: An overview, Food control 79 (2017) 62-73. DIO: 10.1016/j.foodcont.2017.03.027.

[2] R. Beaman, P.W. Morgan, C. Koller, E.L. Wittbecker, E. Magat, Interfacial polycondensation. III. Polyamides, Journal of Polymer Science 40(137) (1959) 329-336. DIO: 10.1002/pol.1959.1204013703.

[3] E.L. Wittbecker, M. Katz, Interfacial polycondensation. VII. Polyurethanes, Journal of Polymer Science 40(137) (1959) 367-375. DIO: 10.1002/pol.1959.1204013707.

[4] T.M. Chang, Sempermeable aqueous microcapsules ("artificial cells"): with emphasis on experiments in an extracorporeal shunt system, ASAIO Journal 12(1) (1966) 13-19.

[5] Y. Shigeri, M. Koishi, T. Kondo, M. Shiba, S. Tomioka, Studies on microcapsules. VI. Effect of variations in polymerization condition on microcapsule size, Canadian Journal of Chemistry 48(13) (1970) 2047-2051. DIO: 10.1139/v70-341.

[6] J. Giro-Paloma, M. Martínez, L.F. Cabeza, A.I. Fernández, Types, methods, techniques, and applications for microencapsulated phase change materials (MPCM): a review, Renewable and Sustainable Energy Reviews 53 (2016) 1059-1075. DIO: 10.1016/j.rser.2015.09.040.

[7] X. Liu, H. Zheng, G. Li, H. Li, P. Zhang, W. Tong, C. Gao, Fabrication of polyurethane microcapsules with different shapes and their influence on cellular internalization, Colloids and Surfaces B: Biointerfaces 158 (2017) 675-681. DOI: 10.1016/j.colsurfb.2017.06.036.

[8] S.A. Guelcher, Biodegradable polyurethanes: synthesis and applications in regenerative medicine, Tissue Eng Part B Rev 14(1) (2008) 3-17. DOI: 10.1089/teb.2007.0133.

[9] X. Liu, S. She, W. Tong, C. Gao, Preparation of elastic polyurethane microcapsules using CaCO 3 microparticles as templates for hydrophobic substances loading, RSC advances 5(8) (2015) 5775-5780. DIO: 10.1039/C4RA12193G.

[10] Y. Niu, F.J. Stadler, J. Song, S. Chen, S. Chen, Facile fabrication of polyurethane microcapsules carriers for tracing cellular internalization and intracellular pH-triggered drug release, Colloids and Surfaces B: Biointerfaces 153 (2017) 160-167. DOI: 10.1016/j.colsurfb.2017.02.018.

[11] Q. Zhang, Y. Shi, X. Zhan, F. Chen, In situ miniemulsion polymerization for waterborne polyurethanes: Kinetics and modeling of interfacial hydrolysis of isocyanate, Colloids and Surfaces A: Physicochemical and Engineering Aspects 393 (2012) 17-26. DOI:10.1016/j.colsurfa.2011.10.016.

[12] Y. Ma, X. Chu, G. Tang, Y. Yao, The effect of different soft segments on the formation and properties of binary core microencapsulated phase change materials with polyurea/polyurethane double shell, Journal of colloid and interface science 392 (2013) 407-414. DOI: 10.1016/j.jcis.2012.10.052.

[13] I. Polenz, S.S. Datta, D.A. Weitz, Controlling the morphology of polyurea microcapsules using microfluidics, Langmuir 30(44) (2014) 13405-13410. DIO: 10.1021/la503234z.

[14] S. Magdassi, Delivery systems in cosmetics, Colloids and Surfaces A: Physicochemical and Engineering Aspects 123 (1997) 671-679. DIO: 10.1016/S0927-7757(97)03792-8.

[15] A. Zoabi, E. Touitou, K. Margulis, Recent Advances in Nanomaterials for Dermal and Transdermal Applications, Colloids and Interfaces 5(1) (2021) 18. DIO: 10.3390/colloids5010018.

[16] K.G. Marra, T.M. Chapman, J.M. Orban, Determination of low critical surface tensions of novel fluorinated poly (amide urethane) block copolymers. 3. Siloxane-containing side chains, Macromolecules 29(23) (1996) 7553-7558. DOI: 10.1021/ma950860d.

[17] N. Rosa, G.V. Martins, M.M. Bastos, J.R. Gois, J.F. Coelho, J. Marques, C.J. Tavares, F.D. Magalhaes, Preparation of robust polyamide microcapsules by interfacial polycondensation of p-phenylenediamine and sebacoyl chloride and plasticization with oleic acid, Journal of microencapsulation 32(4) (2015) 349-357. DOI: 10.3109/02652048.2015.1028494.

[18] W. Zhang, X. Qi, X. Li, Y. Dong, W. Yao, L. Liang, Y. Zhang, Surface modification of polysulfone/PAO40 microcapsules via polydopamine to improve thermal stability and used to prepare polyamide 6-based self-lubricating composite, Colloids and Surfaces A: Physicochemical and Engineering Aspects (2021) 126906. DOI:10.1016/j.colsurfa.2021.126906.

[19] W. Chen, X. Liu, D.W. Lee, Fabrication and characterization of microcapsules with polyamide–polyurea as hybrid shell, Journal of Materials Science 47(4) (2012) 2040-2044. DOI:10.1007/s10853-011-6004-8.

[20] S. D'angelo, P. Galletti, G. Maglio, M. Malinconico, P. Morelli, R. Palumbo, M. Vignola, Segmented poly (ether–ester–amide) s based on poly (l, l-lactide) macromers, Polymer 42(8) (2001) 3383-3392. DOI: 10.1016/S0032-3861(00)00408-0.
[21] F. Quaglia, M.C. Vignola, G. De Rosa, M.I. La Rotonda, G. Maglio, R. Palumbo, New segmented copolymers containing poly (ϵ-caprolactone) and etheramide segments for the controlled release of bioactive compounds, Journal of controlled release 83(2) (2002) 263-271. DOI: 10.1016/s0168-3659(02)00208-0.
[22] M.V. Loureiro, M. Vale, R. Galhano, S. Matos, J.C. Bordado, I. Pinho, A.C. Marques, Microencapsulation of isocyanate in biodegradable poly (ε-caprolactone) capsules and application in monocomponent green adhesives, ACS Applied Polymer Materials 2(11) (2020) 4425-4438. DOI: 10.1021/acsapm.0c00535.
[23] F. Wu, J. Li, H. Quan, J. Han, X. Liu, X. Zhang, J. Yang, Y. Xiang, Robust polyurea/poly (urea–formaldehyde) hybrid microcapsules decorated with Al2O3 nano-shell for improved self-healing performance, Applied Surface Science 542 (2021) 148561. DOI: 10.1016/j.apsusc.2020.148561.
[24] W. Wang, W. Li, L. Song, W. Fan, C. Xiong, X. Gao, X. Zhang, X. Liu, Self-healing performance of coatings containing synthetic hexamethylene diisocyanate biuret microcapsules, Journal of The Electrochemical Society 164(12) (2017) C635. DOI: 10.1149/2.0931712jes
[25] A. Solanki, M. Das, S. Thakore, A review on carbohydrate embedded polyurethanes: An emerging area in the scope of biomedical applications, Carbohydrate polymers 181 (2018) 1003-1016. DOI: DOI: 10.1016/j.carbpol.2017.11.049.
[26] A.R. Solanki, B.V. Kamath, S. Thakore, Carbohydrate crosslinked biocompatible polyurethanes: Synthesis, characterization, and drug delivery studies, Journal of Applied Polymer Science 132(28) (2015). DOI: doi.org/10.1002/app.42223.
[27] A.A. Al-Kahtani, B. Sherigara, Controlled release of diclofenac sodium through acrylamide grafted hydroxyethyl cellulose and sodium alginate, Carbohydrate polymers 104 (2014) 151-157. DOI: 10.1016/j.carbpol.2014.01.018.
[28] Y. Zhang, J. Zheng, W. Ma, X. Zhang, Y. Du, K. Li, Y. Liu, G. Yu, Y. Jia, Ultra-stretchable and ultra-low temperature self-healing polyurethane enabled by dual dynamic bonds strategy, Reactive and Functional Polymers (2022) 105364. DOI: 10.1016/j.reactfunctpolym.2022.105364.
[29] L. Xiao, J. Shi, K. Wu, M. Lu, Self-healing supramolecular waterborne polyurethane based on host–guest interactions and multiple hydrogen bonds, Reactive and Functional Polymers 148 (2020) 104482. DOI: 10.1016/j.reactfunctpolym.2020.104482.
[30] A. O'Donnell, S. Salimi, L. Hart, T. Babra, B. Greenland, W. Hayes, Applications of supramolecular polymer networks, Reactive and Functional Polymers (2022) 105209. DOI: 10.1016/j.reactfunctpolym.2022.105209
[31] P.F. Wiley, The reaction of amides with isocyanates, Journal of the American Chemical Society 71(4) (1949) 1310-1311. DOI: 10.1021/ja01172a047.
[32] G. Dayaker, D. Tan, N. Biggins, A. Shelam, J.L. Do, A.D. Katsenis, T. Friščić, Catalytic Room‐ Temperature C− N Coupling of Amides and Isocyanates by Using Mechanochemistry, ChemSusChem 13(11) (2020) 2966-2972. DOI: 10.1002/cssc.201902576.
[33] F. Gaudin, N. Sintes-Zydowicz, Core–shell biocompatible polyurethane nanocapsules obtained by interfacial step polymerisation in miniemulsion, Colloids and Surfaces A: Physicochemical and Engineering Aspects 331(1-2) (2008) 133-142. DOI:10.1016/j.colsurfa.2008.07.028.
[34] E.M. Maafi, F. Malek, L. Tighzert, P. Dony, Synthesis of polyurethane and characterization of its composites based on alfa cellulose fibers, Journal of Polymers and the Environment 18(4) (2010) 638-646. DOI:10.1007/s10924-010-0218-8.
[35] X. Meng, K.J. Edgar, Synthesis of amide-functionalized cellulose esters by olefin cross-metathesis, Carbohydrate polymers 132 (2015) 565-573. DOI: 10.1016/j.carbpol.2015.06.052.
[36] A. Benkaddour, C. Journoux-Lapp, K. Jradi, S. Robert, C. Daneault, Study of the hydrophobization of TEMPO-oxidized cellulose gel through two routes: amidation and esterification process, Journal of materials science 49(7) (2014) 2832-2843. DOI: 10.1007/s10853-013-7989-y.
[37] E. Lasseuguette, Grafting onto microfibrils of native cellulose, Cellulose 15(4) (2008) 571-580. DOI:10.1007/s10570-008-9200-1
[38] E.S. Dragan, M.M. Lazar, M.V. Dinu, F. Doroftei, Macroporous composite IPN hydrogels based on poly (acrylamide) and chitosan with tuned swelling and sorption of cationic dyes, Chemical engineering journal 204 (2012) 198-209. DOI:10.1016/j.cej.2012.07.126.
[39] R. He, J. Wang, X. Wang, W. Li, X. Zhang, Fabrication and characterization of core–shell novel PU microcapsule using TDI trimer for release system, Colloids and Surfaces A: Physicochemical and Engineering Aspects 550 (2018) 138-144. DOI: 10.1016/j.colsurfa.2018.03.071.
[40] E. Princi, S. Vicini, K. Castro, D. Capitani, N. Proietti, L. Mannina, On The Micro‐ Phase Separation in Waterborne Polyurethanes, Macromolecular Chemistry and Physics 210(10) (2009) 879-889. DOI: 10.1002/macp.200900013.

[41] I. Yilgör, E. Yilgör, G.L. Wilkes, Critical parameters in designing segmented polyurethanes and their effect on morphology and properties: A comprehensive review, Polymer 58 (2015) A1-A36. DOI: 10.1016/j.polymer.2014.12.014.
[42] V. Romanova, V. Begishev, V. Karmanov, A. Kondyurin, M.F. Maitz, Fourier transform Raman and Fourier transform infrared spectra of cross- linked polyurethaneurea films synthesized from solutions, Journal of Raman Spectroscopy 33(10) (2002) 769-777. DOI:10.1002/JRS.914.
[43] L. Jiang, Z. Ren, W. Zhao, W. Liu, H. Liu, C. Zhu, Synthesis and structure/properties characterizations of four polyurethane model hard segments, Royal Society open science 5(7) (2018) 180536. DOI: 10.1098/rsos.180536.
[44] A.S. Giroto, S.F. do Valle, T. Ribeiro, C. Ribeiro, L.H. Mattoso, Towards urea and glycerol utilization as "building blocks" for polyurethane production: A detailed study about reactivity and structure for environmentally friendly polymer synthesis, Reactive and Functional Polymers 153 (2020) 104629. DOI: 10.1016/j.reactfunctpolym.2020.104629.
[45] G. Biemond, J. Feijen, R. Gaymans, Poly (ether amide) segmented block copolymers with adipic acid based tetraamide segments, Journal of applied polymer science 105(2) (2007) 951-963. DOI: 10.1002/app.26202.
[46] J.S. Santana, E.S. Cardoso, E.R. Triboni, M.J. Politi, Polyureas Versatile Polymers for New Academic and Technological Applications, Polymers 13(24) (2021) 4393. DOI: 10.3390/polym13244393.
[47] J. Shang, S. Liu, X. Ma, L. Lu, Y. Deng, A new route of CO 2 catalytic activation: Syntheses of N-substituted carbamates from dialkyl carbonates and polyureas, Green chemistry 14(10) (2012) 2899-2906. DOI: 10.1039/C2GC36043H.
[48] T. Li, C. Zhang, Z. Xie, J. Xu, B.-H. Guo, A multi-scale investigation on effects of hydrogen bonding on micro-structure and macro-properties in a polyurea, Polymer 145 (2018) 261-271. DOI: 10.1016/j.polymer.2018.05.003.
[49] E. Yılgör, I. Yılgör, E. Yurtsever, Hydrogen bonding and polyurethane morphology. I. Quantum mechanical calculations of hydrogen bond energies and vibrational spectroscopy of model compounds, Polymer 43(24) (2002) 6551-6559. DOI:10.1016/S0032-3861(02)00567-0.
[50] M. Kayalvizhi, E. Vakees, J. Suresh, A. Arun, Synthesis and characterization of polyurethane-urea-amide based on functionalized polystyrene, Designed Monomers and Polymers 18(8) (2015) 734-744. DOI: 10.1080/15685551.2015.1070505.
[51] M. Balaban, V. Antić, M. Pergal, I. Francolini, A. Martinelli, J. Đonlagić, The effect of polar solvents on the synthesis of poly (urethane-urea-siloxane) s, Journal of the Serbian Chemical Society 77(10) (2012) 1457-1481. DOI:10.2298/JSC111025056B.
[52] L.H. Staffa, S.H. Bettini, M.A. Chinelatto, Synthesis of Poly (ether- ester- urethane) with a Controlled Molar Mass Based on Poly (ε- caprolactone) and Poly (ethylene glycol) Segments, Macromolecular Symposia, Wiley Online Library, (2020), p. 2000050. DOI: 10.1002/masy.202000050.
[53] B. Mendoza-Novelo, J.L. Mata-Mata, A. Vega-González, J.V. Cauich-Rodríguez, Á. Marcos-Fernández, Synthesis and characterization of protected oligourethanes as crosslinkers of collagen-based scaffolds, Journal of Materials Chemistry B 2(19) (2014) 2874-2882. DOI: 10.1039/C3TB21832E.
[54] J. Qin, J. Jiang, S. Ye, S. Wang, M. Xiao, Y. Tao, G. Jie, Y. Meng, High performance poly (urethane-co-amide) from CO 2-based dicarbamate: An alternative to long chain polyamide, RSC advances 9(45) (2019) 26080-26090. DOI: doi.org/10.1039/C9RA04646A.
[55] I. Kayali, C.K. Jyothi, K. Qamhieh, U. Olsson, Surfactant-free alternative fuel: Phase behavior and diffusion properties, Journal of colloid and interface science 463 (2016) 173-179. DOI:10.1016/j.jcis.2015.10.040.
[56] Y. Ma, Z. Li, H. Wang, H. Li, Synthesis and optimization of polyurethane microcapsules containing [BMIm] PF6 ionic liquid lubricant, Journal of colloid and interface science 534 (2019) 469-479. DOI: 10.1016/j.jcis.2018.09.059
[57] M.L.B. Almeida, E. Ayres, F.C.C. Moura, R.L. Oréfice, Polyurethane foams containing residues of petroleum industry catalysts as recoverable pH-sensitive sorbents for aqueous pesticides, Journal of hazardous materials 346 (2018) 285-295. DOI: 10.1016/j.jhazmat.2017.12.033.
[58] J.M. Budinčić, L. Petrović, L. Đekić, J. Fraj, S. Bučko, J. Katona, L. Spasojević, Study of vitamin E microencapsulation and controlled release from chitosan/sodium lauryl ether sulfate microcapsules, Carbohydrate Polymers 251 (2021) 116988. DOI: 10.1016/j.carbpol.2020.116988.
[59] M. Silva, I. Martins, F. Barreiro, M. Dias, A.E. Rodrigues, Preparation and characterization of poly (urethane–urea) microcapsules containing limonene. Kinetic analysis, International Journal of Polymer Analysis and Characterization 22(8) (2017) 709-724. DOI: 10.1080/1023666X.2017.1369253.
[60] H. Chen, X. Liu, S. Deng, H. Wang, X. Ou, L. Huang, J. Li, C. Jin, Pretilachlor Releasable Polyurea Microcapsules Suspension Optimization and Its Paddy Field Weeding Investigation, Front Chem 8 (2020) 826. DOI: 10.3389/fchem.2020.00826.

[61] R.K. Hedaoo, P.P. Mahulikar, A.B. Chaudhari, S.D. Rajput, V.V. Gite, Fabrication of core–shell novel polyurea microcapsules using isophorone diisocyanate (IPDI) trimer for release system, International Journal of Polymeric Materials and Polymeric Biomaterials 63(7) (2014) 352-360. DOI: 10.1080/00914037.2013.845191.
[62] F. Salaün, G. Bedek, E. Devaux, D. Dupont, L. Gengembre, Microencapsulation of a cooling agent by interfacial polymerization: Influence of the parameters of encapsulation on poly (urethane–urea) microparticles characteristics, Journal of membrane science 370(1-2) (2011) 23-33. DOI: 10.1016/j.memsci.2010.11.033.
[63] S.M. Cakić, I.S. Ristić, O.Z. Ristić, Thermal analysis of polyurethane dispersions based on different polyols, Polyurethane (2012) 79-100. DOI: 10.5772/35800.
[64] E. Julaeha, S. Puspita, D.R. Eddy, T. Wahyudi, M. Nurzaman, J. Nugraha, T. Herlina, J. Al Anshori, Microencapsulation of lime (Citrus aurantifolia) oil for antibacterial finishing of cotton fabric, RSC Advances 11(3) (2021) 1743-1749. DOI: 10.1039/D0RA09314A.
[65] P.H. Campelo-Felix, H.J. Souza, J.A. Figueiredo, R.V. Fernandes, D.A. Botrel, C.R. de Oliveira, M.I. Yoshida, S.V. Borges, Prebiotic Carbohydrates: Effect on Reconstitution, Storage, Release, and Antioxidant Properties of Lime Essential Oil Microparticles, J Agric Food Chem 65(2) (2017) 445-453. DOI: 10.1021/acs.jafc.6b04643.
[66] P.A. Gunatillake, D.J. Martin, G.F. Meijs, S.J. McCarthy, R. Adhikari, Designing biostable polyurethane elastomers for biomedical implants, Australian journal of chemistry 56(6) (2003) 545-557. DOI: 10.1071/CH02168.
[67] G. Trovati, E.A. Sanches, S.C. Neto, Y.P. Mascarenhas, G.O. Chierice, Characterization of polyurethane resins by FTIR, TGA, and XRD, Journal of Applied Polymer Science 115(1) (2010) 263-268. DOI: 10.1002/app.31096.
[68] E. Delebecq, J.P. Pascault, B. Boutevin, F. Ganachaud, On the versatility of urethane/urea bonds: reversibility, blocked isocyanate, and non-isocyanate polyurethane, Chem Rev 113(1) (2013) 80-118. DOI: 10.1021/cr300195n.
[69] F.P. Flores, F. Kong, In vitro release kinetics of microencapsulated materials and the effect of the food matrix, Annual review of food science and technology 8 (2017) 237-259. DOI: 10.1146/annurev-food-030216-025720.
[70] C. Tang, Y. Li, J. Pun, A.S.M. Osman, K.C. Tam, Polydopamine microcapsules from cellulose nanocrystal stabilized Pickering emulsions for essential oil and pesticide encapsulation, Colloids and surfaces A: Physicochemical and engineering aspects 570 (2019) 403-413. DOI: 10.1016/j.colsurfa.2019.03.049.
[71] P.L. Ritger, N.A. Peppas, A simple equation for description of solute release II. Fickian and anomalous release from swellable devices, Journal of controlled release 5(1) (1987) 37-42. DOI: 10.1016/0168-3659(87)90035-6.
[72] L. Ren, B. Huang, W. Fang, D. Zhang, H. Cheng, Z. Song, D. Yan, Y. Li, Q. Wang, Z. Zhou, Multi-encapsulation combination of O/W/O emulsions with polyurea microcapsules for controlled release and safe application of dimethyl disulfide, ACS Applied Materials & Interfaces 13(1) (2020) 1333-1344. DOI: 10.1021/acsami.0c16613.
[73] Q. Huang, S. Gong, W. Han, Y. Chen, X. Shu, Preparation of TTO/UF resin microcapsule via in situ polymerisation and modelling of its slow release, Journal of Microencapsulation 37(4) (2020) 297-304. DOI: 10.1080/02652048.2020.1735548.